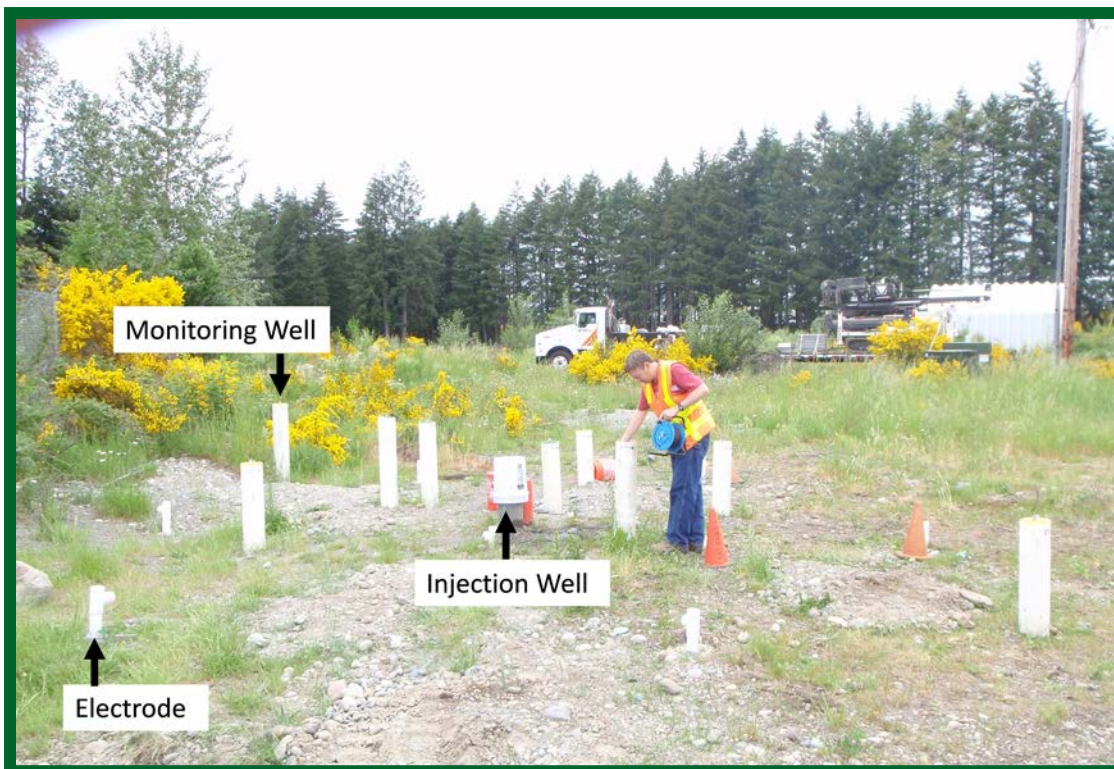


# ESTCP Cost and Performance Report

(ER-200719)



## Combining Low-Energy Electrical Resistance Heating with Biotic and Abiotic Reactions for Treatment of Chlorinated Solvent DNAPL Source Areas

January 2015

*This document has been cleared for public release;  
Distribution Statement A*



ENVIRONMENTAL SECURITY  
TECHNOLOGY CERTIFICATION PROGRAM

U.S. Department of Defense

# COST & PERFORMANCE REPORT

Project: ER-200719

## TABLE OF CONTENTS

	<b>Page</b>
EXECUTIVE SUMMARY .....	ES-1
1.0 INTRODUCTION .....	1
1.1 BACKGROUND .....	1
1.2 OBJECTIVES OF DEMONSTRATION .....	2
1.3 REGULATORY DRIVERS .....	2
2.0 TECHNOLOGY .....	5
2.1 TECHNOLOGY DESCRIPTION .....	5
2.1.1 Low Energy ERH.....	5
2.1.2 In Situ Bioremediation.....	5
2.1.3 ZVI Technology.....	5
2.1.4 Combined Technology.....	6
2.2 ADVANTAGES AND LIMITATIONS OF THE TECHNOLOGY.....	7
3.0 PERFORMANCE OBJECTIVES .....	9
4.0 SITE DESCRIPTION .....	11
4.1 SITE LOCATION.....	11
4.2 SITE GEOLOGY/HYDROLOGY .....	11
4.2.1 Geology.....	11
4.2.2 Hydrology .....	11
4.3 CONTAMINANT DISTRIBUTION.....	12
5.0 TEST DESIGN .....	13
5.1 PHASE 1: BASELINE CHARACTERIZATION .....	13
5.1.1 ISB Test Cell Wells .....	13
5.1.2 ZVI Test Cell Wells .....	13
5.1.3 Treatability and Laboratory Study Results .....	13
5.2 PHASE 2: FIELD DEMONSTRATION OF ISB AND ZVI TREATMENTS WITHOUT ERH .....	15
5.2.1 ISB Injection Strategy.....	15
5.2.2 ZVI Injection Strategy .....	16
5.3 PHASE 3: FIELD DEMONSTRATIONS OF ISB AND ZVI TREATMENTS WITH ERH.....	18
5.3.1 ERH Operations .....	18
5.3.2 Sampling Methods .....	18
5.4 RESULTS PHASE 2 AND 3: ISB .....	18
5.5 RESULTS PHASE 2 AND 3: ZVI.....	25
5.6 PHASE 3: LOW-ENERGY ERH .....	29

## TABLE OF CONTENTS (continued)

	<b>Page</b>
6.0 PERFORMANCE ASSESSMENT .....	33
6.1 MASS BALANCE FACTORS ISB.....	35
6.1.1 ISB Enhanced Mass Transfer.....	35
6.1.2 ISB Impact of Elevated Temperature on Kinetics .....	37
6.2 MASS BALANCE FACTORS ZVI.....	38
6.2.1 ZVI Mass Transfer.....	38
6.2.2 ZVI Kinetic Changes .....	41
6.2.3 Biotic/Abiotic.....	43
6.2.4 Impact of Temperature on Dissolution/Volatilization .....	43
6.3 SUMMARY OF PERFORMANCE RELATED TO OBJECTIVES .....	44
7.0 COST ASSESSMENT.....	47
7.1 COST MODEL.....	47
7.2 COST DRIVERS .....	52
7.2.1 ZVI.....	52
7.2.2 ISB .....	56
7.2.3 Thermal.....	58
7.3 COST ANALYSIS.....	58
8.0 IMPLEMENTATION ISSUES .....	59
9.0 REFERENCES .....	61
APPENDIX A       POINTS OF CONTACT.....	A-1

*This page left blank intentionally.*

## LIST OF FIGURES

		<b>Page</b>
Figure 1.	Treated NAPL areas in relation to the test site. ....	12
Figure 2.	Final placement of ISB and ZVI test cells – February 2013.....	14
Figure 3.	Typical progression of redox parameters during Phase 2 and 3. ....	20
Figure 4.	Phase 2 and 3 total molar VOC mass in ISB test cell (A) and downgradient concentration at ISB-MW4 (B).....	22
Figure 5.	Phase 2 and 3 total VOC mass flux (A), reductive daughter product mass flux (B) and VOC, daughter product and chloride discharge (C) as a function of temperature across the ISB-MW1 and ISB_MW2 transect. ....	23
Figure 6.	TCE vapor flux during Phase 1, 2 and 3 for ISB test cell.....	26
Figure 7.	cis-DCE vapor flux during Phase 1, 2 and 3 for ISB test cell. ....	26
Figure 8.	VC Vapor Flux during Phase 1,2 and 3 for ISB Test Cell.....	27
Figure 9.	Total VOC mass within the ZVI test cell.....	28
Figure 10.	Soil concentrations of TCE, DCE, and VC measured before ZVI treatment Nd at the end of Phase 2 and Phase 3. ....	30
Figure 11.	Cumulative energy and temperature in ZVI and ISB test cells. ....	30
Figure 12.	Average external ZVI test cell TMP temperatures. ....	31
Figure 13.	Average external ISB test cell TMP temperatures.....	31
Figure 14.	Mass-discharge analysis configuration where $MD_{in}$ is the influent mass discharge and $MD_{out-w}$ and $MD_{out-v}$ are the effluent mass discharge in the water and vapor phases, respectively.....	34
Figure 15.	Linear correlation between MDdissolution, R, and $R_{tc}$ as a function of temperature. ....	37
Figure 16.	Calculated TCE reaction rates and Nd for the INJ segment. ....	40
Figure 17.	Chloride concentration over time in the ZVI test cell.....	42
Figure 18.	ZVI cost model treatment area and system infrastructure. ....	48
Figure 19.	ISB cost model treatment area and system infrastructure.....	49
Figure 20.	Treatment time comparison. ....	51

## LIST OF TABLES

		<b>Page</b>
Table 1.	Safe drinking water act maximum contaminant levels for Ft. Lewis EGDY contaminants of concern. ....	3
Table 2.	Performance objectives. ....	9
Table 3.	Summary of baseline analytical results from field screening and soil sampling. ....	15
Table 4.	Summary of amendment injections in the ISB test cell during Phase 2 and 3. ....	16
Table 5.	Summary of ZVI injection parameters. ....	16
Table 6.	Hydraulic parameters calculated based on the tracer test and used for calculations. ....	17
Table 7.	ZVI sample types and quantities. ....	19
Table 8.	Summary of mass discharge estimates for Phase 2 and 3. ....	23
Table 9.	TCE and temperature profiles for ISB-MW1. ....	24
Table 10.	Modeled results for TCE for ISB-MW1. ....	25
Table 11.	Average groundwater concentration of TCE and dechlorination products. ....	29
Table 12.	Comparison of mass discharge from the ISB test cell in groundwater and in soil gas. ....	36
Table 13.	Average overall rate of TCE transformation based on organic dechlorination products ( $R_t$ ) and chloride concentrations ( $R_{cl}$ ) (Truex et al., 2011). ....	43
Table 14.	Summary of achievement of demonstration performance objectives. ....	44
Table 15.	Cost assumption model. ....	50
Table 16.	Cost model assumptions and costs for low-temperature ZVI. ....	53
Table 17.	Cost model assumptions and costs for low-temperature ISB. ....	55
Table 18.	Cost model assumptions and costs for high-temperature thermal. ....	57

*This page left blank intentionally.*

## ACRONYMS AND ABBREVIATIONS

---

CFR	Code of Federal Regulations
COD	chemical oxygen demand
DCE	dichloroethene
DHC	Dehalococcoides spp.
DNA	deoxyribonucleic acid
DNAPL	dense non-aqueous phase liquid
DO	dissolved oxygen
DoD	U.S. Department of Defense
EGDY	East Gate Disposal Yard
EOS <sup>®</sup>	emulsified oil substrate
EPA	U.S. Environmental Protection Agency
ERH	electrical resistance heating
ESTCP	Environmental Security Technology Certification Program
gpm	gallons per minute
ISB	in situ bioremediation
JBLM	Joint Base Lewis-McChord
mmol	millimole
MROD	Mount Rainer Ordnance Detail
MVS	Mining Visualization System
MW	monitoring well
NAPL	non-aqueous phase liquid
O&M	operations and maintenance
ORP	oxidation-reduction potential
PCE	tetrachloroethene
PCU	power control unit
PID	photoionization detector
POL	petroleum, oils, and lubricants
ppm	parts per million
qPCR	quantitative polymerase chain reaction
RI	remedial investigation
SV	soil vapor
TCA	1,1,1-trichloroethane
TCE	trichloroethylene



## ACRONYMS AND ABBREVIATIONS (continued)

---

TMP	temperature monitoring point
TRS	Thermal Remediation Services
uM	micromoles per liter
USACE	United States Army Corps of Engineers
VC	vinyl chloride
VOC	volatile organic compound
ZVI	zero valent iron

## ACKNOWLEDGEMENTS

*Technical material contained in this report has been approved for public release.  
Mention of trade names or commercial products in this report is for informational purposes only;  
no endorsement or recommendation is implied.*

*This page left blank intentionally.*

## **EXECUTIVE SUMMARY**

### **BACKGROUND**

The applicability of in situ groundwater remedies such as in situ bioremediation (ISB) or zero valent iron (ZVI) reduction in chlorinated solvent source zones (i.e., containing dense non-aqueous phase liquids [DNAPLs]) is often limited by the relatively long treatment timeframes required to meet remedial objectives at sites. Conceptually, the goal of this project was to evaluate moderate heating (i.e., 35-50 °C) to accelerate the dissolution and desorption of residual trichloroethylene (TCE) contamination as well as accelerating the in situ degradation kinetics, and to minimize volatilization and therefore the need for soil gas extraction and treatment, as is typically required for high-temperature thermal applications. This field demonstration combined electrical resistance heating (ERH) with ZVI and ISB for TCE treatment in two separate test cells. The demonstration objectives included quantifying 1) the effect of low-energy heating on the extent and rate of contaminant degradation, 2) the impacts on the mass removal rate, 3) the relative contributions of biotic and abiotic contaminant degradation mechanisms at different temperatures, and 4) the costs and benefits of applying low-energy heating with in situ treatments.

### **TECHNOLOGY DESCRIPTION**

ERH technology is used to treat soil and groundwater contamination, and can be especially effective in treating TCE and other volatile organic compound (VOC) contaminant sources in the DNAPL phase. ERH increases subsurface temperatures to the boiling point of water at which point, steam is created in situ and contaminants are directly volatilized, extracted and treated in above-ground treatment systems. ISB is a demonstrated technology that relies on amendment injections to grow bacteria capable of dechlorinating chloroethenes. ZVI technologies rely on emplacement of ZVI in situ to facilitate abiotic reductive elimination reactions of chlorinated solvents, which does not generate hazardous degradation products. Combining subsurface heating (ERH) with in situ treatments (ISB or ZVI) has the potential to accelerate treatment rates of the in situ technologies because higher temperatures increase degradation reaction rates, and also increase the DNAPL dissolution and contaminant desorption rates, which are often the rate-limiting steps in DNAPL treatment with these technologies.

### **DEMONSTRATION RESULTS**

This project, located at the East Gate Disposal Yard at Joint Base Lewis-McChord near Tacoma, WA, was conducted in three phases. Phase 1 consisted of initial characterization and verification of the suitability of ISB and ZVI test cells to meet project objectives. Phase 2 consisted of a field demonstration of ISB and ZVI without heating to establish the performance of the individual technologies at ambient temperatures. Phase 3 consisted of field demonstrations of low-energy ERH combined with ISB and ZVI at temperatures.

In the ZVI test cell Phase 2 field demonstration, micron-scale ZVI particles were suspended within a shear-thinning fluid to increase their distribution within the subsurface. Approximately 190 kg of 2-micron-diameter ZVI particles were injected into the top six feet (ft) of an

unconfined aquifer within the TCE DNAPL source zone, and were successfully distributed over 12 ft from the injection well. All monitoring wells (MWs) showed indications of dechlorination including partial dechlorination products, and high concentrations of ethene and ethane, by the end of two month monitoring period at ambient temperature. Data indicated a mixture of abiotic reactions and biotic dechlorination reactions were occurring, as the daughter products included cis-dichloroethene (DCE) (biotic) but not vinyl chloride, and ethene and ethane (which probably resulted from abiotic processes).

For the ISB test cell, efficient degradation of TCE was established during Phase 2 via monthly injections of emulsified vegetable oil and powdered whey into the injection well for nine months. A reactive treatment zone was established where geochemical conditions were generally reduced to support methane production and reductive dechlorination of TCE to primarily cis-DCE with trace ethene was achieved at ambient temperature. However, relatively high groundwater velocities within the treatment zone resulted in relatively low retention of the amendments within the test cell, which was the reason that monthly injections were conducted.

Phase 3 was started at the same time in both the ISB and ZVI test cells by applying ERH to raise the temperature in the test zone to the target temperatures (30°C - 45°C and 40°C - 55°C respectively). The elevated temperatures increased the dissolution of contaminant into the groundwater and increased the rate and extent of dechlorination in both test cells. During this demonstration the total contaminant mass discharge increased by a factor of 4-16 within the ZVI test cell, and consisted primarily of the reductive daughter products (ethene and ethane), as the degradation kinetics were sufficiently high to keep the TCE concentrations low. For the ISB test cell, the total contaminant mass discharge increased by a factor of approximately 4-5 and the fraction of the total mass present as ethene increased dramatically during Phase 3 compared to Phase 2. In both test cells, the contaminant fluxes to the vadose zone increased by less than 1.5% at the elevated temperatures compared to ambient, indicating VOC losses to the vadose zone were minimal and vapor recovery and treatment likely would not be needed.

## **BENEFITS**

A detailed review of the costs for low-temperature ZVI and ISB suggests that low-temperature heating is less expensive than high temperature ERH, but only incrementally so. Therefore, application of low-temperature heating combined with in situ treatment likely makes sense only for sites that contain relatively low to moderate VOC concentrations as residual DNAPL, so that the contaminant mass could be removed in less than 1-2 years of treatment. Sites with higher concentrations or significantly pooled DNAPL probably cannot be treated effectively using low-temperature heating. However, the benefit of heating to accelerate in situ reactions was clearly demonstrated, and therefore, combining in situ treatment with heating may be beneficial, especially for sites already considering high temperature heating. In addition, in situ technologies could be implemented after thermal shutdown, to rapidly degrade any remaining contaminants in the treatment zone while the subsurface temperature remains elevated.

## 1.0 INTRODUCTION

This report describes results of a field demonstration combining low energy electrical resistance heating (ERH) with in situ bioremediation (ISB), or with iron-based reduction using zero valent iron (ZVI), for the remediation of dense non-aqueous phase liquid (DNAPL) source zones. The field demonstration was conducted at Joint Base Lewis-McChord (JBLM) Landfill 2, formerly known as the Fort Lewis East Gate Disposal Yard (EGDY). This report is focused on demonstrating the benefits of combining low-energy ERH with either ISB or with iron-based reduction using injectable ZVI, including the assessment of the extent to which contaminant degradation is enhanced during heating compared to ambient temperatures, the relative contribution of biotic and abiotic contaminant degradation mechanisms at different temperatures, and the cost-benefit of applying low-energy heating with in situ treatments. The demonstration was conducted in three phases to allow accurate evaluation of the effects of ERH on ISB and ZVI reduction. The ISB and ZVI tests were conducted in hydraulically isolated test cells in the following three phases:

- Phase 1: Pre-characterization and verification of the suitability of each test cell to meet demonstration objectives, treatment system installation, and baseline sampling.
- Phase 2: Field demonstration of ISB and ZVI (without low-energy ERH).
- Phase 3: Field demonstration of ISB and ZVI (with low-energy ERH).

## 1.1 BACKGROUND

Chlorinated solvents are the most prevalent contaminants detected at hazardous waste sites according to the U.S. Environmental Protection Agency (EPA) National Priorities List. The U.S. Department of Defense (DoD) alone has approximately 3,000 sites contaminated with chlorinated solvents, with a large percentage of these sites containing residual sources of contamination containing DNAPLs, which serve as, long-term sources of dissolved phase groundwater contamination.

The prevalence of chlorinated solvents has been linked to both to their widespread use and to their longevity in the environment. Their longevity is partly due to the hydrophobic nature that makes them such good solvents, as well as their relatively oxidized states that prevent them from serving as electron donors for microorganisms. In addition, the solubility of common chlorinated solvents is relatively low, which plays a significant role in limiting mass transfer to the aqueous phase once the solvents contaminate groundwater. Dissolution of a DNAPL into groundwater is governed by the difference between the aqueous solubility of the compound and the actual concentration in groundwater. Due to the laminar flow nature of most groundwater systems, very little mixing of water occurs, even a few centimeters from the DNAPL; thus, there is limited dissolution of DNAPLs into groundwater. The result is that chlorinated solvents can persist in groundwater for many decades.

The prevalence of DNAPL sites has prompted the DoD's Strategic Environmental Research and Development Program (SERDP) and Environmental Security Technology Certification Program (ESTCP) program to develop a technical review panel focused on developing a strategy for research, the development of cost-effective technologies, and the implementation of existing

source zone treatment technologies, namely enhanced ISB, in situ iron-based reduction using ZVI, and thermal treatment using ERH.

Although ERH, ISB, and ZVI are relatively mature technologies, the benefits of combining these technologies have not been fully demonstrated or validated. This combined technology approach is expected to provide more rapid source area cleanup than the ambient temperature in situ technologies alone but without the high cost of conventional ERH associated with boiling the entire water column and extracting and treating contaminants at the surface.

## 1.2 OBJECTIVES OF DEMONSTRATION

To evaluate the potential for decreased costs and increased efficiency of the combined remedies, the specific technical objectives of this demonstration are as follows:

- **Objective 1:** To validate the rate and extent to which contaminant degradation is increased during enhanced ISB at a temperature of approximately 30 to 40°C compared to ISB at ambient temperature.
- **Objective 2:** To validate the rate and extent to which contaminant degradation is increased during iron-based reduction using injectable ZVI at a temperature of approximately 50 to 60°C compared to ambient temperature.
- **Objective 3:** To determine the relative contributions of biotic and abiotic degradation at different temperatures in order to optimize each.
- **Objective 4:** To use data collected from a controlled field demonstration at a DoD site to develop cost and performance data for the combined remedies.

The goal of using heating to enhance in situ reactions is to treat a source area more cost effectively than is possible with only heating (e.g., ERH) or only an in situ remediation technology (e.g., ISB). A key data need for determining how to meet this goal is in finding the “sweet spot” where the cost of heating is offset by the gains in treatment efficiency for the in situ remediation technology. The demonstration provided a controlled field setting to test the impact of increased temperature on treatment efficiency using these in situ technologies. The demonstration also provided key engineering data relative to how ERH can be cost-effectively designed and applied to provide moderate heating rather than the standard design for heating to the boiling point.

## 1.3 REGULATORY DRIVERS

As stated in Section 1.1, chlorinated solvents are the most prevalent contaminants detected at hazardous waste sites. The solubilities of the common chlorinated solvents (tetrachloroethene [PCE], trichloroethylene [TCE], 1,1,1-trichloroethane [TCA], and carbon tetrachloride) range from about 200 to 1,400 milligrams per liter (mg/L) at 25°C (Sale, 1998). These solubilities exceed Federal Safe Drinking Water Act maximum contaminant levels (see Table 1) by five to six orders of magnitude. The persistence of chlorinated solvents in groundwater, their prevalence, and their solubilities far in excess of health-based levels drive the need for cost-effective remediation technologies.

**Table 1. Safe drinking water act maximum contaminant levels for Ft. Lewis EGDY contaminants of concern.**

<b>Compound</b>	<b>Regulatory Limit (<math>\mu\text{g/L}^1</math>)</b>
PCE	5
TCE	5
cis-DCE	70
trans-DCE	100
Vinyl chloride	2

<sup>1</sup>40 CFR 141.61



*This page left blank intentionally.*

## 2.0 TECHNOLOGY

ERH, ISB, and ZVI are described below with emphasis on information pertinent to application of combined treatment/heating configurations. The demonstration described in this report was the first field test for the combination of ISB/ERH and ZVI/ERH.

### 2.1 TECHNOLOGY DESCRIPTION

#### 2.1.1 Low Energy ERH

Thermal treatment through ERH is a proven aggressive technology for the treatment of DNAPL, and other contaminant source zones, by increasing subsurface temperatures to the boiling point of water. At this temperature, steam is created in situ and contaminants are directly volatilized. The steam acts as a carrier gas to strip volatiles from the subsurface and route them to the surface under vacuum for treatment. However, high capital and maintenance costs and the requirement for vapor control and secondary waste treatment make this technology a high cost alternative at many contaminated sites. The low-energy ERH approach discussed here is based on raising subsurface temperatures to approximately 30 to 60°C to enhance the rate of biotic and abiotic contaminant dechlorination, respectively. This less aggressive approach will use electrodes installed on a wider spacing using boring, pile-driving, or direct push technology and will eliminate vapor and steam recovery and treatment with potential for 50 to 75% reduction in costs.

#### 2.1.2 In Situ Bioremediation

ISB for chlorinated ethenes has been investigated, demonstrated, and implemented at numerous sites, including non-aqueous phase liquid (NAPL) Area 3 of Landfill 2 at JBLM. Biostimulation techniques use injection of amendments as electron donors to grow indigenous or bioaugmented bacteria capable of dechlorinating chloroethenes. The added value of increasing temperatures may not only enhance dissolution of DNAPLs, but *biological reaction rates also increase with increasing temperature*. Microbial activity is a function of temperature, and for mesophilic microorganisms, which include *Dehalococcoides ethenogenes* (Empadinhas et al., 2004) as well as other dehalogenators (Suyama et al., 2002), optimal metabolic rates are typically near 30 to 40°C, which ERH can stimulate (Heath and Truex, 1994).

#### 2.1.3 ZVI Technology

ZVI has been developed and applied for in situ remediation of inorganic compounds and chlorinated solvents. Abiotic reductive elimination reactions facilitated by ZVI are beneficial for treatment of chlorinated contaminants, such as TCE, because no persistent hazardous degradation products are generated. ZVI reactions can also directly and indirectly generate dichloroethene (DCE), vinyl chloride (VC) and ethene through facilitation of biotic reductive dechlorination. Initial kinetics of TCE dechlorination by ZVI are relatively fast and have been studied as a function of temperature (Su and Puls, 1999), TCE concentration (Orth and Gillham, 1996; Grant and Kueper, 2004), type of iron (Miehr et al., 2004; Lin and Lo, 2005; Ebert et al., 2006), and presence of multiple chlorinated solvents and other organic and inorganic species (Dries et al., 2004; Dries et al., 2005; D'Andrea et al., 2005). While initial kinetics of ZVI

reactions are relatively fast, reaction kinetics can diminish over time due to corrosion and mineral precipitation, and the rate and extent of decrease in reaction rates are a function of groundwater chemistry (Farrell et al., 2000; D'Andrea et al., 2005; Kohn and Roberts, 2006).

#### **2.1.4 Combined Technology**

In situ technologies destroy contaminants without generation of secondary waste streams, are non-hazardous to workers and the environment, have relatively low capital and maintenance costs, and generally minimize disturbance of the site. The remedial timeframe using many in situ technologies, however, is relatively long due to limitations in mass transfer of contaminants from the residual to the dissolved phase, where contaminants are available for destruction. Combining subsurface heating with in situ treatment has the potential to accelerate mass transfer further and to enhance remediation performance because higher temperatures can increase degradation reaction rates, dissolution, and volatilization. The rate of both biologically-mediated reactions and ZVI reactions are expected to increase from temperatures typical of most groundwater systems (10-12EC) to reach a maximum and then decline with further temperature increase. This type of temperature function is well documented for microbial processes (Atlas, 1987; Empadinhas, 2004; Suyama, 2002), and for reductive dechlorination reactions in particular (Kohring, 1989; Holliger, 1993; He, 2003), and was observed for ZVI dechlorination processes. Note that the rate of some reactions, such as hydrolysis, may also continue to increase with increasing temperature.

Contaminant dissolution and volatilization generally increase with increasing temperature (Yaws, 2009; Sleep, 1997; Horvath, 1982). Typical thermal treatment applications increase temperatures to near the boiling point and mobilize DNAPL through generation of vapors which are extracted and treated. Imhoff 1997 empirically and predicatively demonstrated that moderate temperature applications of hot water flushing for chlorinated solvent treatment enhance the mass transfer rate of residual DNAPL by a factor of four to five when temperatures were increased from 5°C to 60°C. In providing thermally enhanced ISB or ZVI treatment, dissolution of DNAPL would be enhanced by the following phenomena:

1. At elevated temperatures, the dissolution rate of DNAPL is increased compared to lower temperatures. For the proposed technology, it is important to maximize dissolution of DNAPL while minimizing volatilization so that the contaminants are transferred and maintained in the aqueous phase (where in situ reactions occur), but not transferred to the gas phase (where they must be captured to avoid spread of contamination).
2. At elevated temperatures, the desorption rate is increased compared to lower temperatures; improving the availability of these contaminants for degradation.

This combined technology approach is expected to provide more rapid source area cleanup than the ambient temperature in situ technologies alone but without the high cost of conventional ERH associated with boiling the entire water column and extracting and treating contaminants at the surface. For this approach to be viable, however, increases in physical mass transfer rates for both dissolution and volatilization as temperature increases must be balanced by reaction or contaminants will migrate out of the heated treatment zone without being degraded.

## 2.2 ADVANTAGES AND LIMITATIONS OF THE TECHNOLOGY

Factors significantly affecting cost and performance of this technology include:

- **Ability to identify the NAPL or sediment-associated contaminants and adequately deliver electron donor or ZVI.** Site-specific properties, including depth, permeability and heterogeneity of the formation, and NAPL/sediment-associated contaminant distribution, can be assessed by performing a baseline characterization to identify the adequate numbers of electron donor and/or ZVI injection wells in the source area and/or the correct volumes and/or concentrations of amendments to be used to achieve adequate contact. Wells may be screened or packers installed to target selected intervals for amendment delivery.
- **Ability to treat large source mass.** Both ZVI and ISB would have a limited overall capacity for source treatment. Zones with high NAPL saturation would require a high dosing of ZVI or ISB substrates and long treatment times. In those cases, other treatment approaches may be more cost effective.
- **Presence/absence of a microbial community capable of complete conversion of TCE to ethene (ISB test cell).** This factor can be assessed through baseline sampling for the presence/absence of VC and ethene; or through molecular evaluation of the microbial community, including quantitative polymerase chain reaction (qPCR) for *Dehalococcoides* spp., the only group of bacteria known to reduce cis-DCE, and VC. This factor may be addressed through bioaugmentation.

There are significant advantages of coupling low energy thermal treatment with either ISB or ZVI injections relative to implementing each of these technologies alone. These include:

- **Minimal above ground infrastructure**—The coupling of in situ technologies with moderate heating negates the need for above ground treatment systems generally necessary for conventional thermal applications.
- **Lower safety hazards**—Moderate heating also has the advantage of minimizing safety hazards associated with high temperature heating of the subsurface.
- **Low risks**—The remediation strategies take advantage of in situ treatment where most or all of the contaminant treatment occurs in the soil or groundwater, thereby reducing risks to human health and the environment during implementation compared to ex situ technologies.
- **Low secondary waste generation**—Most of the contaminant treatment occurs on-site, with little off-site disposal of residuals required. In addition, secondary treatment usually associated with thermal treatment (i.e., soil vapor (SV) extraction and ex-situ treatment) will not be required.
- **Lower cost**—The cost assessment from the field demonstration showed moderate cost increases by adding heating infrastructure for low-temperature applications, in addition, the technology can be coupled to high temperature thermal applications where much of the infrastructure is already available.

- **Overall risk reduction**—Demonstration data show that heating-enhanced ZVI and ISB can achieve moderate treatment endpoint conditions for groundwater and sediment contamination.

These technologies, however, face several limitations, including:

- **Greater uncertainty in treatment performance and life cycle costs.** Uncertainties are inherent with in situ processes because conditions throughout the entire targeted region cannot be explicitly manipulated to create conditions that are optimal for the desired in situ reaction at all locations in the subsurface.
- Site-specific conditions can limit application of many in situ remedial technologies, including complex lithology, low permeability media, and/or complex geochemistry.

### 3.0 PERFORMANCE OBJECTIVES

As previously stated, the overall objective of this demonstration was to evaluate the cost-benefit of applying low-energy ERH in combination with ISB and iron-based reduction technologies using injectable ZVI. With this in mind, detailed performance objectives were developed for each phase of the demonstration that will help meet the overall objective. Table 2 outlines the overall qualitative and quantitative performance objectives for the demonstration. It is important to note that interpretation of the data relies on a comparison of the reaction kinetics and evaluation of mass balance components in soils, soil gas, and groundwater (including contaminants and reductive daughter products) between Phases 2 and 3 in each individual cell. This approach avoids the difficulties in interpretation that would be introduced due to unknown differences in hydrogeologic heterogeneity and DNAPL distribution if ambient and heating tests were conducted in separate locations.

The contaminant degradation rate data was measured and used to estimate treatment timeframe. This information was then used to develop a life-cycle cost estimate, including capital and operating costs and a present value assessment, so that overall remediation costs for the ambient and heated treatments can be effectively compared (see Section 7).

**Table 2. Performance objectives.**

Type of Performance Objective	Primary Performance Criteria	Expected Performance (Metric)	Actual Performance Objective Met?
Qualitative	Induce dechlorination of chlorinated ethenes.	Dechlorination to desired endpoints will be achieved in each test cell.	Complete degradation to innocuous endpoints demonstrated in each test cell.
	Reduction in parent compounds and accumulation of abiotic and/or biotic reductive daughter products.	<p>Biotic contaminant removal will be the primary mechanism at ambient and elevated temperature in the ISB test cell.</p> <p>Abiotic and biotic contaminant removal will be significant in the ZVI test cell at ambient temperature; however, abiotic mechanisms will predominate at elevated temperature.</p>	<p>Biotic contaminant removal primary mechanisms in ISB test cell.</p> <p>Both abiotic and biotic contaminant removal in ZVI test cell, but complete dechlorination to ethene/ethane demonstrated primarily through abiotic pathway at ambient and elevated temperatures.</p>

**Table 2. Performance objectives (continued).**

<b>Type of Performance Objective</b>	<b>Primary Performance Criteria</b>	<b>Expected Performance (Metric)</b>	<b>Actual Performance Objective Met?</b>
<b>Quantitative</b>	Characterize nature of contamination with test cell.	Sufficient contaminant mass will be present in both test cells to meet demonstration objectives.	<p>ISB: initial TCE soil concentration averaged 32 mg/kg with maximum concentrations of 130 mg/kg near ISB-MW2.</p> <p>ZVI: initial TCE soil concentration averaged 10 mg/kg with maximum concentrations of 115 mg/kg near INJ, estimated 1 kg total TCE in test cell.</p>
	Define rate of dechlorination as a function of temperature.	The rate of dechlorination will be enhanced at elevated temperature in both test cells relative to ambient temperature.	<p>ISB: average (avg) ambient rate= 1600 mmol/d (VOC data) to 6100 mmol/d (Cl data). Avg rate during T&gt;30C= 3600 mmol/d (VOC data) to 10,700 mmol/d (Cl data).</p> <p>ZVI: (INJ data) avg ambient rate = 1 mmol/d (organic data) to 1.2 (Cl data) average rate at T&gt;30C = 4.5 mmol/d (organic data) to 9.7 mmol/d (Cl data).</p>
	Quantify test cell mass balance and loss mechanisms for chlorinated ethenes in the test cells as a function of temperature.	Contaminant mass removal will be enhanced at elevated temperature in both test cells relative to ambient temperature.	<p>ISB: TCE treatment rate increased by a factor of 4.6 at T=40C compared to 10C based on empirical correlation. Volatilization accounted for &lt;1.45% of losses.</p> <p>ZVI: TCE mass loss = 9 mg/kg with 85% of loss at T&gt;30C with volatilization accounting for &lt; 1% of losses based on modeling.</p>
	Evaluate cost-effectiveness of heating.	The overall treatment efficiency at elevated temperature will be enhanced sufficiently to offset the cost of heating in both test cells.	<p>ISB cost (3 years)=\$599</p> <p>ISB+ heat (1.8 years)=\$567</p> <p>ZVI cost (3 years)= \$626</p> <p>ZVI+heat cost (1.3 years) = \$632</p> <p>High Temp. Thermal (0.2 years)=\$692</p>

## **4.0 SITE DESCRIPTION**

### **4.1 SITE LOCATION**

Construction at the Logistics Center site began in 1941 with construction of the Quartermaster Motor Base, which was renamed the Mount Rainier Ordnance Depot (MROD) in 1942. It operated until 1963, furnishing ordnance supplies, maintenance and rebuilding services for Fort Lewis until 1963. In 1963, the MROD was turned over to the Logistics Center to serve as the primary non-aircraft maintenance facility for the post.

TCE was used as a degreasing agent at this facility until the mid-1970s, when it was replaced with TCA. Waste TCE was co-disposed with waste oils at several locations. Landfill 2, also known as EGDY, was used between 1946 and 1960 as a disposal site for waste generated at the MROD. Trenches were excavated in the yard and reportedly received TCE and petroleum, oils, and lubricants (POL) from cleaning and degreasing operations. These materials were transported to the Landfill 2 in barrels and vats from the various use areas; about six to eight barrels per month of waste TCE and POL may have been disposed. These materials were also used to aid in burning other wastes.

### **4.2 SITE GEOLOGY/HYDROLOGY**

#### **4.2.1 Geology**

At least three glacial and three non-glacial units have been identified in the sediments occurring above sea level at the Landfill 2. The Vashon Glacial Drift deposit, consists of glacial deposits including recessional outwash, till and ice contact deposits, advance outwash and glaciolacustrine silt/clay. The recessional outwash is present in the vertical extent of the demonstration area, consisting of interbedded brown to gray sandy gravel and sand with minor silt intervals. At the top of the recessional outwash is an intensely iron oxide-stained Third Glacial Drift, containing orange to dark gray sand gravel and sand with minor silt interbeds.

Holocene-Anthropomorphic Deposits are present in the trench areas and consist of man-made fill that include debris and burned material. A Pre-Olympia Drift is also present with gray to brown, fine-to medium-grained sand with minor sandy gravel interbeds. The Second Non-Glacial deposits contain mottled, massive, organic rich, clayey, sandy gravel (mudflows) or lavender silt, peat, sand, and gravelly sand (fluvial overbank deposits) while the Third Non-Glacial deposit only contains lavender silt, peat, sand, and gravelly sand. For more detailed information of the glacial and non-glacial units refer to the Final ER-0719 Report (CDM Smith, 2012).

#### **4.2.2 Hydrology**

The Vashon Aquifer or Upper Aquifer is the primary aquifer in the demonstration area. The Vashon drift, Olympia beds, and Pre-Olympia drift comprise the Vashon unconfined aquifer. Vashon till and Olympia beds may act locally as discontinuous aquitards within the Vashon aquifer. Vashon outwash and pre-Olympia drift deposits comprise the aquifer materials within the Vashon aquifer. The Vashon aquifer varies in thickness from 100 – 130 ft and is continuous throughout the Landfill 2.



### 4.3 CONTAMINANT DISTRIBUTION

The test site is located within the 13.5-acre portion of the Landfill 2 containing the vast majority of former disposal trenches and wastes. Principal contaminants included TCE and daughter products and POL from cleaning and degreasing operations. Thermal remediation via ERH occurred at the three highest-concentration TCE-containing NAPL areas between 2003 and 2007 to reduce source mass significantly and ultimately to reduce the overall clean-up time frame of the plume. None of the three treated areas are within the direct hydraulic path of the test site, although NAPL Area 3 is approximately 250 ft downgradient and west of the site. Figure 1 shows the treated NAPL areas in relation to the test site. Remedial investigation (RI) borings were conducted to investigate NAPL areas with high TCE concentrations. Locations RS0060 and RS0062 indicated positive NAPL readings as well as high TCE concentrations (Figure 1).

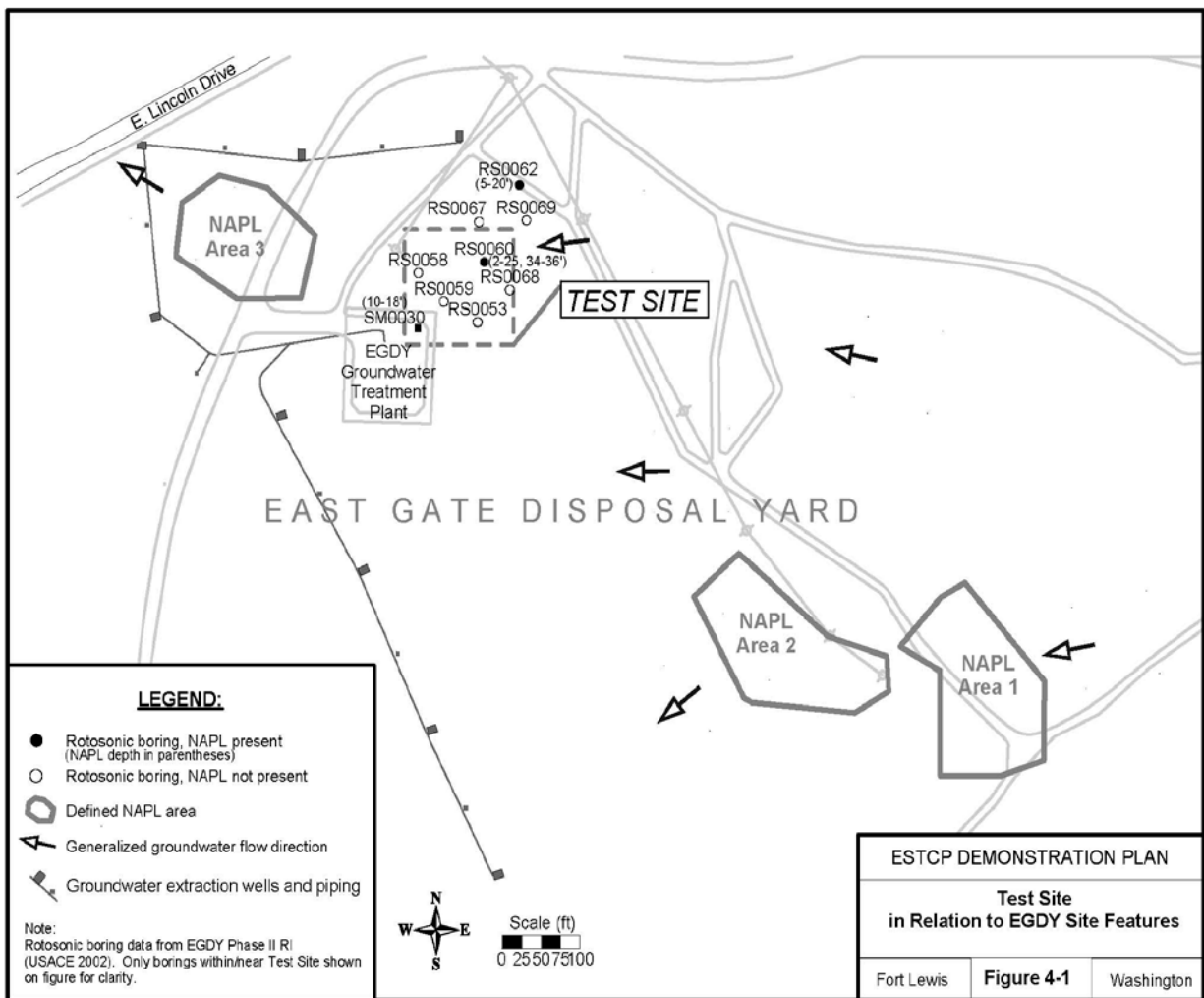


**Figure 1. Treated NAPL areas in relation to the test site.**

## **5.0 TEST DESIGN**

### **5.1 PHASE 1: BASELINE CHARACTERIZATION**

Phase 1 of the demonstration included a pre-design characterization to determine the suitability of the test cells for the demonstration. The characterization effort included testing to confirm presence of sufficient residual DNAPL mass within the test cells; test cell installation, baseline contaminant characterization via groundwater sampling, soil gas sampling, and soil boring and sampling; a Gore Sorber Survey, and hydraulic tracer testing. As mentioned above, the selection of the planned test cells (RS0060 and RS0062) was based on positive NAPL readings with high TCE concentrations (Figure 1). Details of the Gore Sorber Survey, boring logs, well completion details, and tracer study design are provided in the Final ER-0179 Report and not repeated here (CDM Smith, 2012). Specifics of the characterization activity and the objectives of the activity can be found in Table 5-1 on page 31 of the Final ER-0179 Report. ISB Test Cell Wells.

#### **5.1.1 ISB Test Cell Wells**

Field screening results from the pre-characterization and Gore Sober Survey indicated both ISB-MW1 and ISB-MW3 locations contained sufficiently high levels of contamination (see Figure 2 for location of actual well placements). Soil sample depths and analytical results are presented in Table 3. A detailed hydraulic evaluation was also conducted for the ISB test cell. Details of this testing are provided in the Final ER-0719 Report (CDM Smith 2012) and not repeated here. A summary of the resultant estimates for groundwater seepage velocity and hydraulic gradient are shown in Table 6.

#### **5.1.2 ZVI Test Cell Wells**

Field results from the, pre-design characterization, showed significant TCE soil concentrations at the injection well, ZVINJ1 (Figure 2). Table 3 presents results of the soil characterization activities within the ZVI test cell area. A tracer study was also conducted at the ZVI test cell just prior to injection of ZVI to evaluate the injection hydraulic response, finalize ZVI injection parameters, and to evaluate groundwater flow velocity through elution monitoring. Results of the ZVI tracer test are discussed in conjunction with the ZVI injection results in Section 5.2.2 (see also Truex 2010). Refer to Figure 2, for the final test cell layout for both ISB and ZVI test sites.

#### **5.1.3 Treatability and Laboratory Study Results**

Laboratory tests were conducted to 1) finalize selection of the polymer as the delivery mechanism for the ZVI, 2) determine injection parameters (i.e., quantity of ZVI/polymer addition), and 3) provide baseline reaction kinetics to assist in field data interpretation. The laboratory tests demonstrated that SlurryPro™ does not impact the dechlorination rate of TCE by ZVI in the presence of site sediments, or the solubility of TCE (Truex et al., 2010).

The mass of TCE within the targeted ZVI treatment zone was estimated to be 2 to 6 kg-TCE, with the highest concentration of TCE centered around the injection well. A target ZVI injection of 150kg was selected based on the average and maximum stoichiometry observed in the laboratory treatability tests. The full treatability test report is provided in the Final ER-0719 Report (CDM Smith, 2012). Table 5.8, page 52 of the Final ER-0719 Report, shows the results of the laboratory treatability tests that were used to calculate the ZVI mass to be injected.

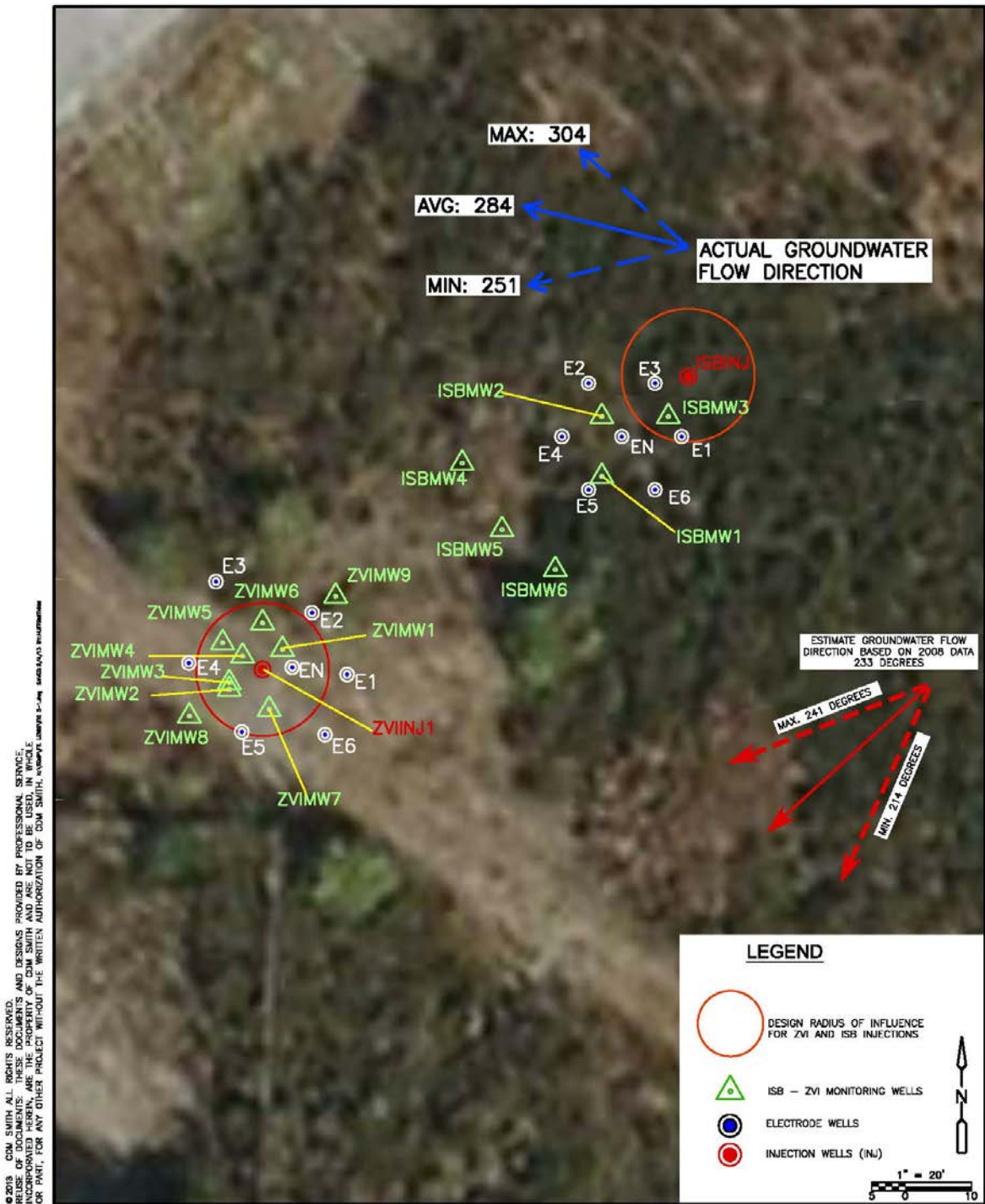


Figure 2. Final placement of ISB and ZVI test cells – February 2013.

**Table 3. Summary of baseline analytical results from field screening and soil sampling.**

Cell	Borehole Location	Analytical Sample Point (ft bgs)	Analytical Result TCE (µg/kg)	Analytical Result cis-1,2-DCE (µg/kg)	Maximum PID Measurement (ppm)	Interpreted NAPL Depth Interval
ISB	ISB-MW1	17.5	76,000	11	715	16.5-20 ft bgs
		19	10,000	5.6	98	
		27.5	4,900	28	44	
	ISB-MW2	9	5,100	11	63	14.0-20 ft bgs
		14	130,000	91	1,555	
		19	65,000	30	9,300	
	ISB-MW3	9	17,000	8	197	None
		14.5	8,500	7.9	142	
		16	4,000	16	2,662	
ZVI	ZVI-INJ1	8.8	220,000	180	629	5-13 ft bgs
		10.5	11,000	110	15	
		15.3	6,800	48	4	
	ZVI-MW1	11	2500	38	10.6	None
		16	470	33	0.7	
		20.5	250	16	0.7	
	ZVI-MW2	12	1600	100	32.9	None
		16.5	1400	34	1.4	
		20	1900	110	9.8	

Note: Area shaded in grey indicates soil samples that met the “Go” decision criteria of 10,000 µg/kg. The grey areas that also have bold lettering indicate samples collected within the saturated interval and gray areas without bold lettering indicate samples collected within the vadose zone.

## 5.2 PHASE 2: FIELD DEMONSTRATION OF ISB AND ZVI TREATMENTS WITHOUT ERH

This demonstration evaluated performance of the ISB and ZVI in situ technologies at ambient groundwater temperatures. Phase 2 activities for the ISB test cell included establishing efficient anaerobic reductive dechlorination at ambient temperature through injection of electron donors emulsified oil substrate (EOS<sup>®</sup>) and then whey powder, as well as tracking the rates for dechlorination. Phase 2 activities for the ZVI test cell included first establishing in situ destruction of TCE using injectable micron-scale ZVI (see Truex 2010 for details) and then tracking the transformation reactions that convert TCE to ethene and ethane via beta-elimination. Reaction rate times for ISB and ZVI in Phase 2 were compared to rate times in Phase 3 in order to establish the effect ERH on in situ biodegradation. A full description of the Phase 2 test design is in the Final ER-0719 Report (CDM Smith 2012).

### 5.2.1 ISB Injection Strategy

Results from the first two EOS<sup>®</sup> injections suggested that the EOS<sup>®</sup> was not retained within the test cells following either EOS<sup>®</sup> injection in sufficient quantity to drive anaerobic conditions. Therefore, a decision to switch from EOS<sup>®</sup> to buffered why injection was made. For the remainder of Phase 2 and Phase 3 a total of nine sodium bicarbonate-buffered why injections

were completed at the ISB-INJ well. The injection volume and mass of whey and sodium bicarbonate for each injection event is summarized in Table 4.

**Table 4. Summary of amendment injections in the ISB test cell during Phase 2 and 3.**

<b>Phase/ Injection Event</b>	<b>Injection Type</b>	<b>Injection Dates</b>	<b>Total Volume Injected (gallons)</b>	<b>Volume EOS (gal) or Mass whey (lb)</b>	<b>EOS (% v/v) or whey (% w/w)</b>	<b>% w/w bicarbonate</b>
Phase 2/ 2 Events	EOS	5-Feb-09/10-Mar-09	3608	115.5	1.36-3.50%	NA
Phase 2/ Events	Powdered whey/ bicarbonate	3-Jun-09/21-Jul-09	2743	400	1.72-1.79%	0.86-0.89%
Phase 3/ Events	Powdered whey/ bicarbonate	10-Sep-09 – 2-Mar-10	8170	1200	1.35-1.98%	0.68-0.99%

### 5.2.2 ZVI Injection Strategy

Prior to ZVI injection, a sodium bromide (100 mg/L as bromide ion) solution was injected to evaluate the injection pressure, bromide distribution within the targeted test zone, and to enable monitoring of bromide elution to estimate the groundwater velocity at the test site. Tracer concentrations were monitored in the test cell wells to define the tracer breakthrough and elution responses. Table 5 summarizes the ZVI injection parameters. A full description of the ZVI injection process is described in Truex 2011.

**Table 5. Summary of ZVI injection parameters.**

<b>Item</b>	<b>Value</b>
Water injection rate(average)	20.5 gpm
SlurryPro™ injection rate(average)	2.2 gpm
Surfactant injection rate (average)	76 mL/min
Total solution injection rate (average)	22.7 gpm
Total injection solution volume	13,660 L
SlurryPro™ stock solution injection volume	1300 L
Injected ZVI mass	187 kg
SlurryPro™ concentration (average)	0.019 wt%
Surfactant concentration (average)	0.0008 wt%
ZVI concentration in injection solution	1.36 wt%
Injection duration	158 min

**Table 6. Hydraulic parameters calculated based on the tracer test and used for calculations.**

**Landfill 2, Fort Lewis, Washington: ISB Test Cell**

Monitoring Point	Distance from Injection Point (ft)	Depth of Screen (ft bgs)	Tracer Travel Time <sup>1</sup> (minutes)	Groundwater Velocity During Tracer Test (ft/d)	Estimated Ambient Groundwater Velocity (ft/d)	Estimated Horizontal Hydraulic Gradient During Tracer Test <sup>2</sup>	Estimated Effective Porosity <sup>3</sup>	Hydraulic Conductivity <sup>3</sup> (ft/d)
INJ	0	5 - 19	--	--	--	--	--	--
MW1-3	21	12	440	67	31	0.028	0.18	455
MW1-4	21	17	310	95	36	0.034	0.18	532
MW1-5	21	22	430	69	32	0.028	0.18	466
MW1-6	21	27	460	64	31	0.027	0.18	452
MW2-3	15	12	240	87	28	0.040	0.18	413
MW2-4	15	17	250	84	27	0.040	0.18	397
MW2-5	15	22	150	139	45	0.040	0.18	661
MW2-6	15	27	NA	NA	NA	NA	NA	NA
MW3-3	7	12	50	202	66	0.040	0.18	958 <sup>5</sup>
MW3-4	7	17	70	144	47	0.040	0.18	684 <sup>5</sup>
MW3-5	7	22	40	252	82	0.040	0.18	1,197 <sup>5</sup>
MW3-6	7	27	>1573	NA	NA	NA	NA	NA

Notes:

<sup>1</sup> Tracer travel time is defined as the time from midpoint of the bromide injection period to the time of breakthrough at the monitoring point.

<sup>2</sup> The hydraulic gradient is estimated based on the gradient observed during the whey injection event that occurred in cell in 2009 and 2010.

<sup>3</sup> Literature derived porosity estimate (Vermeul et al. 2000).

<sup>4</sup> The hydraulic conductivity (K) is calculated as  $K = (\text{Groundwater Velocity} \times \text{effective porosity}) / \text{horizontal hydraulic gradient}$

NA - Not analyzed due to no measurable response

<sup>5</sup> Hydraulic conductivities estimated for MW3 were not used in modeling of mass discharge because of uncertainty in their representativeness due to tracer arrival times that occurred before the tracer injection had ended.

### **5.3 PHASE 3: FIELD DEMONSTRATIONS OF ISB AND ZVI TREATMENTS WITH ERH**

Phase 3 of the demonstration evaluated the effect of low-temperature heating of the test cells to 30 - 40°C for the ISB cell and 40 - 50°C for the ZVI test cell. Again, groundwater, soil gas, and soil boring and sampling data were collected, which allowed for the measurement of the heated condition (Phase 3) compared to the ambient condition (Phase 2) (see Trues 2011 for details). Both the ISB and ZVI test cells employed 7 electrodes each located as shown in Figure 5-1. Each electrode location consisted of a single 12-foot electrode element which is connected to the surface via a high temperature electrical cable.

#### **5.3.1 ERH Operations**

The ERH operations period for Phase 3 include site activities from system shakedown and start-up through ERH operations and system demobilization. Treatment of the ZVI test cell ran from June 17, 2009 to March 22, 2010 with temperatures maintained between 31 and 48°C. During this period a total of 60,038 kilowatt hour (kWh) of energy was applied to the ZVI treatment region. Treatment of the ISB test cell ran from September 26, 2009 to March 22, 2010 with temperatures maintained between 25 and 36°C. During this period a total of 33,330 kWh of energy was applied to the ISB treatment region. Detail regarding startup and safety checks, operations and demobilization is provided in the Final ER-0719 Report (CDM Smith, 2012).

#### **5.3.2 Sampling Methods**

Samples, including groundwater, soil gas and soils were collected from all three phases in the ZVI and ISB test cell. The total number and types of samples taken can be found in the Final ER-0719 Report (CDM Smith, 2012). A summary of Phase 2 and Phase 3 samples and locations is provided in Table 7. Measurement of subsurface temperatures occurred at temperature monitoring point (TMPs) locations located upgradient, within, and downgradient of both of the ISB and ZVI test cells. These TMPs were used to track the heating process and ensure that the desired subsurface temperatures were achieved and maintained.

A detailed description of TMP placement and results can be found in the Final ER-0719 Report (CDM Smith 2012). Tables 5-11 and 5-12 in the Final ER-0719 Report show the TMP thermocouple numbers and depth for ZVI and ISB test cells respectively.

### **5.4 RESULTS PHASE 2 AND 3: ISB**

Following Phase 2 EOS<sup>®</sup> and whey injections, geochemical conditions were established that are favorable to reductive dechlorination. Redox conditions shifted in accordance with the nutrient distribution. The conditions within the ISB test cell and approximately 36 feet (ft) downgradient were methanogenic from approximately four months after the first EOS<sup>®</sup> injection.

#### ***Carbon Distribution***

The distribution of electron donor injected (EOS<sup>®</sup> and whey) was monitored by measuring the chemical oxygen demand (COD) concentrations at the injection and MWs. The COD

concentration in the treatment zone averaged 8 mg/L right after the first injection. Thirty days after the first injection and just before the second injection, COD concentrations ranged from 25 – 180 mg/L. Following Phase 2 injections with whey, COD concentrations were maintained at approximately, 42-270 mg/L within the ISB test cell. During Phase 3 concentrations were slightly lower overall with values ranging from 0-170 mg/L. For a complete table of COD concentrations within the ISB test cell during Phase 1-3 see Table 5-19, page 83, of the Final ER-0719 Report (CDM Smith, 2012).

**Table 7. ZVI sample types and quantities.**

Demonstration Technology	Phase	Groundwater Samples/ Locations	Soil Gas (Summa) Samples/ Locations	Soil Gas (Gore Sorbers) Samples/Locations	Soil Samples/ Locations
ZVI	2	10 <sup>1</sup> / INJ, MW1-MW9	5 <sup>2</sup> / MW2, MW4, MW5, MW6, MW7	6 <sup>3</sup> / MW2, MW4, MW6, Flux A, Flux B, Flux C	6 <sup>4</sup> / Soil Cores near INJ, MW1
	3	160 <sup>1</sup> / INJ, MW1-MW9	35 <sup>2</sup> / MW2, MW4, MW5, MW6, MW7	18 <sup>3</sup> / MW2, MW4, MW6, Flux A, Flux B, Flux C	9 <sup>4</sup> / Soil Cores near INJ, MW1
ISB	2	78 <sup>5</sup> / INJ, MW1-MW6	6 <sup>2</sup> / MW1-3	24 <sup>3</sup> / MW1-3, Flux A, Flux B, Flux C	9 <sup>4</sup> / Soil Cores
	3	88 <sup>5</sup> / INJ, MW1-MW6	11 <sup>2</sup> / MW1-3	18 <sup>3</sup> / MW1-3, Flux A, Flux B, Flux C	9 <sup>4</sup> / Soil Cores

- (1) VOCs by EPA 8260B, RSK-175 (ethene, ethane, and acetylene), EPA 300 (Anions include Cl-, Br-, SO<sub>4</sub><sup>2-</sup>, F-, and NO<sub>3</sub>-), Field parameters include ferrous iron, Br- and/or I- DO, oxidation reduction potential (ORP), conductance, and temperature. QPCR for microbial populations for samples collected from MW2 and MW4.
- (2) TO-15 Analysis for VOCs and ethene, ethane, acetylene.
- (3) Gore Solids Analysis for VOC, hydrocarbon, ethane, ethene, acetylene.
- (4) VOCs by EPA 8260B
- (5) VOCs by EPA 8260B, RSK-175 (ethene, ethane, and acetylene), EPA 300 (Anions include Cl-, Br-, SO<sub>4</sub><sup>2-</sup>, F-, and NO<sub>3</sub>-), COD, Field parameters include ferrous iron, Br- and/or I- DO, ORP, conductance, and temperature. QPCR for microbial populations for samples collected from MW2 and MW4.

### **Geochemical Response**

Chlorinated hydrocarbons serve as electron acceptors in microbially-mediated redox reactions during reductive dechlorination. During bioremediation, injection of nutrients in sufficient quantities drives redox conditions from aerobic → nitrate reducing → iron reducing → sulfate reducing → methanogenic. Reductive dehalogenation, dechlorination of PCE and TCE to cis-1,2-DCE generally occurs under iron-reducing to sulfate-reducing conditions. Complete dechlorination to ethene typically occurs under sulfate-reducing to methanogenic conditions. Dissolved Oxygen (DO) concentrations were reduced from to less than 0.5 mg/Ls considered optimal for dechlorination. Nitrate concentrations were never a significant factor in the reaction processes at this Site. Baseline Ferrous Iron concentrations were initially observed at 0.4 mg/L, but increased to 2 – 4 mg/L after Phase 2 injections. Anything above 1 mg/L is considered optimal for dechlorination. Sulfate concentrations were substantially depleted from baseline concentrations of 14 – 22 mg/L to below 0.5 mg/L after the first donor injection, and remained depleted through Phase 3 indicating the establishment of sulfate reducing conditions.

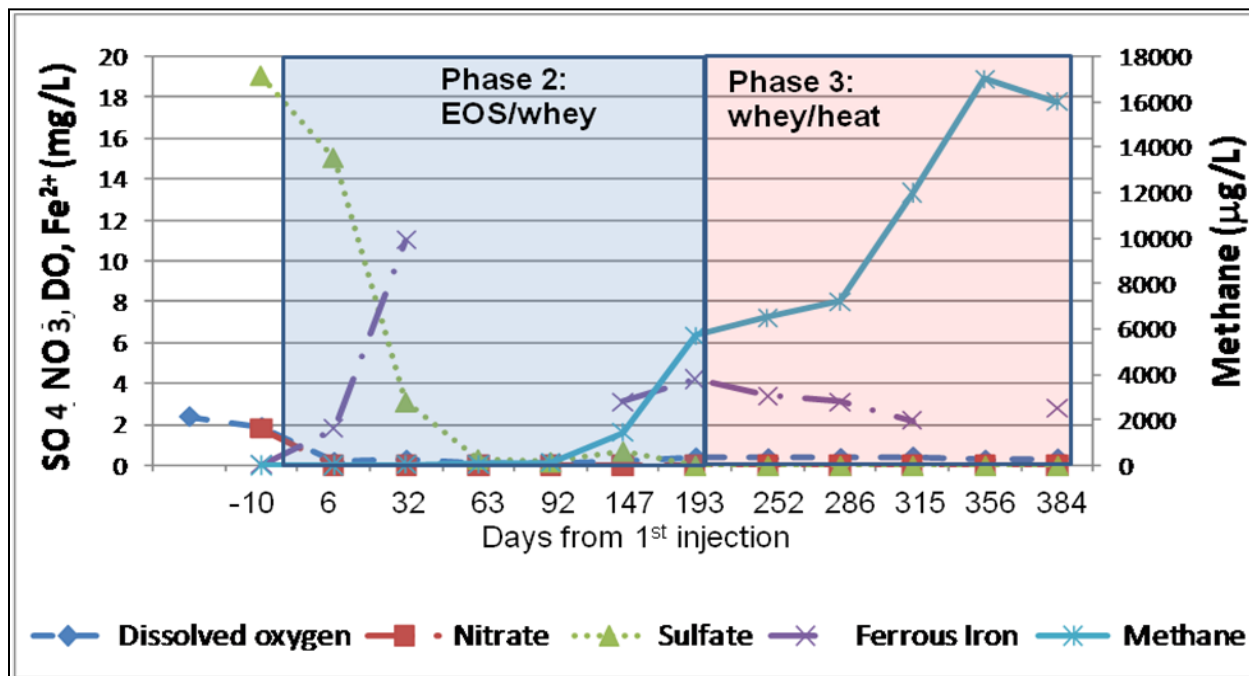
The pH of groundwater plays a significant role in the activity of dechlorinating bacteria (DHC). Activity of DHC decreases significantly in aquifers with pH less than 6.0, and they are



completely inactive below pH of 5.5. Therefore pH was adjusted using buffers so it remained was above 6.0 for all monitoring locations within and downgradient of the ISB test cell for Phases 2 and 3.

Methane concentrations above 500 micrograms per liter ( $\mu\text{g/L}$ ) are considered optimal for dechlorination. Methane concentrations were generally either very low ( $<2 \mu\text{g/L}$ ) or non-detect during baseline sampling, but increased following nutrient injection, with substantial concentrations of  $4100 \mu\text{g/L}$  to  $6300 \mu\text{g/L}$  within the ISB test cell and ranged from  $340 \mu\text{g/L}$  to  $720 \mu\text{g/L}$  downgradient of the test area at the end of Phase 2. During Phase 3, methane concentration continued to dramatically increase with concentrations greater than  $10,000 \mu\text{g/L}$  observed. These data indicate that strongly methanogenic conditions were developed during Phase 2 and 3. Figure 3 illustrates typical methane concentrations over time for the ISB test cell.

**Figure 3. Typical progression of redox parameters during Phase 2 and 3.**



### Contaminant Degradation

Carbon and redox parameters are only indicators of conditions favorable for reductive dechlorination at the Site. The concentrations of parent compounds (TCE) and reductive daughter products (DCE, VC, ethene, ethane and chloride) were used as direct evidence of treatment of contaminants of concern at the site. During Phase 2, the TCE concentrations declined, and near stoichiometric conversion to cis-DCE. VC was periodically observed (see Figure 4). In addition, low levels of ethene were also observed.

As shown in Figure 4, during Phase 3, the concentration of DCE, VC and ethene dramatically increased, as did chloride. However, along with significant increases in daughter products, large increases in TCE were also observed. The maximum volatile organic compound (VOC) concentrations observed corresponded to the time when the maximum temperatures were

observed in the test cell, December, 2009 (day 314) indicating a dramatic increase in VOC loading to groundwater. During Phase 3, however, a significant shift in products was also observed at the downgradient wells (Figure 4). Initially, a large increase in DCE was observed at ISB-MW4, but then decreased by the November, 2009 (day 286) sampling event. By March and April, a combination of TCE, DCE, VC and ethene were observed at ISB-MW4. Figure 4 presents the percentage of total mass of VOCs (sum of TCE, cis-1, 2-DCE, VC and ethene) and daughter products (DCE, VC, and ethene) as TCE for small volumes around each MWs ISB-MW1, ISB-MW2, and ISB-MW3 during Phases 2 and 3. Total concentrations increased by a factor of 3-4 after heating began compared to concentrations observed just prior to heating. Figure 5 illustrates the total VOC flux compared to flux of reductive daughter products.

### ***Mass Flux and Discharge Modeling***

Groundwater hydraulic and contaminant data were input into the Mining Visualization System (MVS) Version 9.52 software to evaluate mass discharge from the test cell over time during Phase 2, after reducing conditions had been established, and in Phase 3.

The seepage velocity module was used to compute a vector groundwater flow field. The module outputs vector data representing X, Y, and Z components. The total molar VOC and degradation daughter product mass flux and discharge data was used to evaluate the relative change in mass flux and discharge. These values can be found in Table 5-23, page 92 Final ER-0719 Report (CDM Smith, 2012). The MVS-modeled discharge from the ISB-MW1 and -MW2 transect prior to heating (n=3 sampling events May, July, and August 09), was 1.8 mole/day corresponding to approximately 240 g of TCE/day (Table 8). After heating, the average mass discharge for all 7 post-heating events was 4.8 mole/day, corresponding to 633 g/day of TCE, a factor of 2.6 increase in mass discharge. The maximum mass discharge observed during the sampling event corresponding to maximum temperature observed in the test cell (December, day 314) was 7.2 mol/d corresponding to approximately 943 g/d of TCE, a factor of 3.9 increase in mass discharge. This enhanced mass transfer occurred in the test cell during heating and is primarily attributed to the heating effects (i.e. accelerated dissolution and kinetics). It is assumed that contaminant flux coming into the test cell is negligible since VOC concentrations at ISB-INJ upgradient of the test cell were generally 2-4 orders of magnitude lower than concentration observed at ISB-MW1, -MW2 or -MW3. Therefore, it was assumed that all of the contaminants were derived from residual source material within the test cell itself.

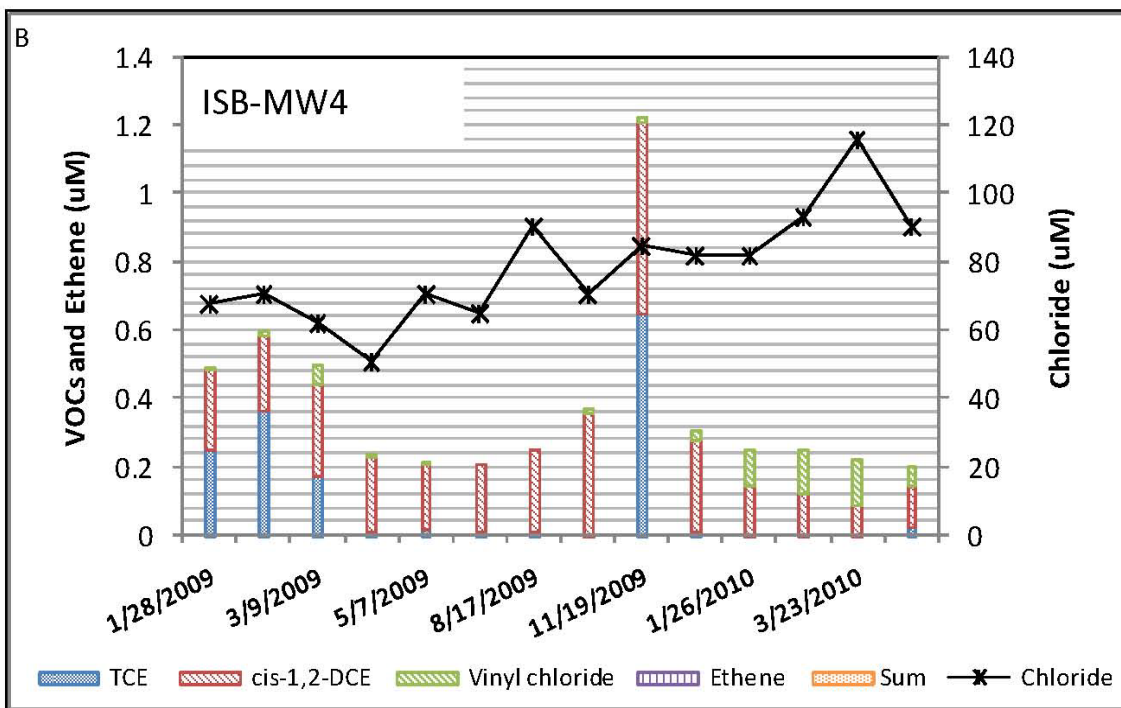
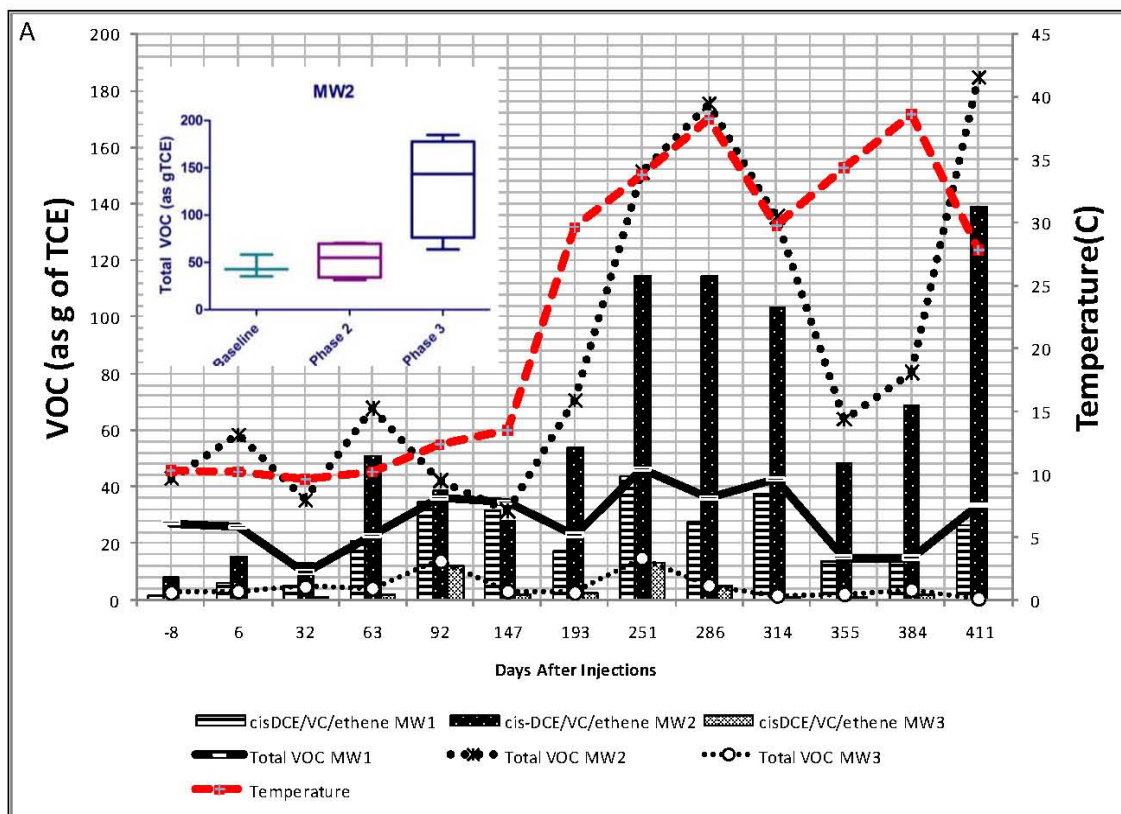


**Figure 4. Phase 2 and 3 total molar VOC mass in ISB test cell (A) and downgradient concentration at ISB-MW4 (B).**

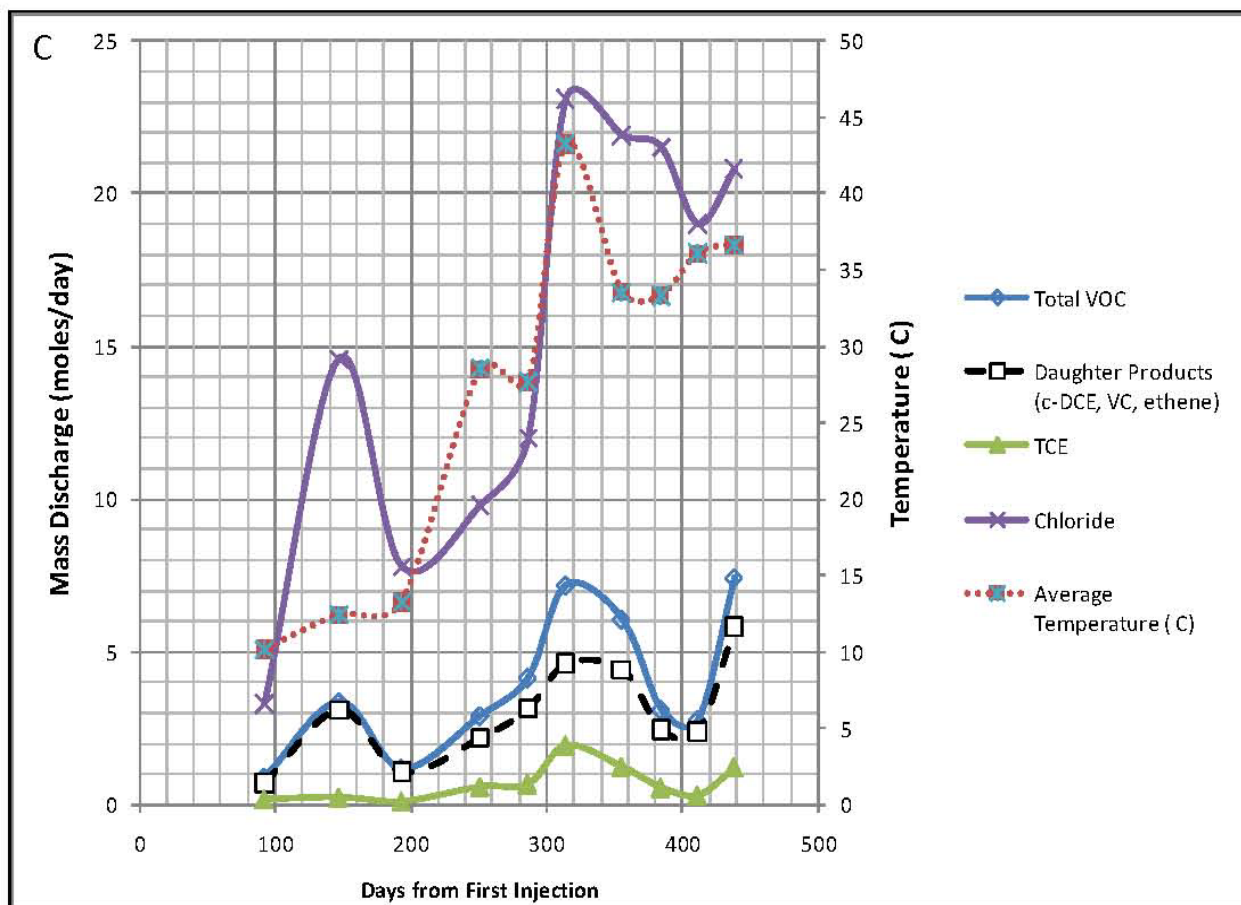


**Figure 5. Phase 2 and 3 total VOC mass flux (A), reductive daughter product mass flux (B) and VOC, daughter product and chloride discharge (C) as a function of temperature across the ISB-MW1 and ISB\_MW2 transect.**

**Table 8. Summary of mass discharge estimates for Phase 2 and 3.**

MD <sub>out</sub>	Phase 2			Phase 3				
	Average mole/day (n=3) <sup>a</sup>		gTCE/day <sup>b</sup>	Average mole/day (n=7) <sup>a</sup>		gTCE/day <sup>b</sup>		
Total VOC	1.8	+/-	1.3	240	4.8	+/-	2.0	633
Products (cis-DCE, VC, ethene)	1.6	+/-	1.3	214	3.6	+/-	1.4	471
Chloride	6.1	+/-	5.7	798	10.7	+/-	3.8	1403

Notes:

<sup>a</sup> Concentrations from all of the MWs were kriged to determine a 3D contaminant plume. Mass discharge was evaluated through a transect 15.8 ft across through ISB-MW1 and -MW2 and 21 ft deep.

<sup>b</sup> g of TCE per day was evaluating by multiplying the molar concentration of Total VOCs or the sum of cis-DCE, VC and ethene by the molecular weight of TCE. TCE dechlorinated based on chloride data was evaluated by taking the chloride molar concentration and subtracting the background chloride (2.5 moles) and then multiplying by the molecular weight of TCE. It was assumed that 1 mole of chloride corresponded to 1 mole of TCE dechlorinated as cis-DCE was the predominant by-product

In addition to total VOCs, mass discharge of daughter products from the test cell was evaluated to determine the biodegradation efficiency within the heated zone. Of the 240 g/day of TCE-equivalent VOC mass discharged from the test cell 214 g/day or 89% was observed as daughter products during Phase 2. This was primarily DCE (89-99% of the molar mass of daughter products DCE, VC and ethene during the August 09 event). During Phase 3, total molar daughter products increased to an average of 471 g/d TCE-equivalent treated, a factor increase of 2.2. Again, DCE was the primary degradation product (13-98%), although significant quantities of VC and ethene were also observed at many locations. The maximum discharge of daughter products occurred during the December (day 314) event, which increased to 607 g/d as TCE, or 64% of the total VOC discharge.

In addition to daughter products, mass discharge using chloride was also evaluated. If applicable, chloride is generally more conservative compared to a molar mass balance using organic degradation by products in groundwater because chloride is conserved in groundwater, while organic VOCs can be degraded (especially VC and ethene/ethane which are very transient within the Landfill 2 shallow aquifer once generated), can partition to the soil, and/or can volatilize to the vadose zone. Biodegradation and volatilization can result in underestimating organic VOC concentrations, and ultimately TCE reactions, when only groundwater data are considered. At Landfill 2, background chloride around the test cell was averaged 70.6 micromoles per liter (uM)(average of ISBINJ, ISB-MW4 through –MW6 during baseline). This was used as the background and subtracted from the concentrations observed during the active portion of Phase 2 and Phase 3. The adjusted chloride concentrations were input into the MVS model to evaluate TCE dechlorination. The average chloride flux during Phase 2 was 6.2 moles/day compared to 15.8 moles/day during heating which corresponds to an average of 798 g/d of TCE dechlorinated to DCE during Phase 2 and 2078 g/d of TCE dechlorinated to DCE during Phase 3.

### ***Soil Vapor Monitoring***

As part of the mass balance approach, an evaluation of heating on increased volatilization of contaminants to the vadose zone and ultimately to the ground surface and potential overlying buildings was conducted. Details regarding the modeling, assumptions, and calibration are included in the Final ER-0719 Report (CDM Smith, 2012). Table 9 presents an example model input for TCE and temperatures profiles for MW-1 during the January, August, and December sampling events, and a monitoring point four months into ERH-enhanced bioremediation, with the highest recorded average in situ temperatures.

**Table 9. TCE and temperature profiles for ISB-MW1.**

<b>Month</b>	<b>TCE GW Conc (µg/L)</b>	<b>GW Temp (°C)</b>	<b>Temp of Capillary Fringe (°C)</b>	<b>Temp of Unsaturated Zone (°C)</b>
January	14,000	10.1	10	7
August	27	11.6	13	17
December	1600	45.2	41	18

Using these data as a starting point, the following steps are calculated for each sample event: TCE  $C_{\text{source}}$ , TCE  $D_{\text{eff}}$  for the entire soil column, and finally the TCE flux from groundwater to ground surface. Table 10 presents the modeled results. This procedure was repeated for all of the test cell MWs.

**Table 10. Modeled results for TCE for ISB-MW1.**

Month	$C_{\text{source}}$ ( $\mu\text{g/L}$ )	$D_{\text{eff}}$ ( $\text{cm}^2/\text{sec}$ )	Flux ( $\mu\text{g}/\text{sec}/\text{cm}^2$ )
January	2870	$1.05 \times 10^{-4}$	$9.87 \times 10^{-7}$
August	5.99	$1.06 \times 10^{-4}$	$2.08 \times 10^{-9}$
December	1514	$1.16 \times 10^{-4}$	$5.78 \times 10^{-7}$

Figures 6, 7, and 8 illustrate the change in flux for TCE, DCE, and VC, respectively, based on bioremediation treatment during Phase 2 (July and August 2009) and Phase 3 (August to December 2009). The figures also include groundwater temperatures for the modeled flux rates. When ISB was conducted alone, TCE flux generally declined by two orders of magnitude as reductive dechlorination reduced the mass of TCE, and fluxes of DCE and VC increased as the mass of daughter compounds increased as a result of biodegradation in groundwater. During Phase 3, the flux of TCE and DCE increased by approximately two orders of magnitude as increases in system temperature increased dissolution and volatilization of the contaminants. The flux of VC increased by as much as three orders of magnitude because VC was almost non-existent in the system prior to ISB and therefore reductive dechlorination greatly increased the mass of VC more so than another daughter compound. Increases in mass flux to the vadose zone were most dramatic after the onset of heating (November 2009), but generally declined over time. These results indicate dechlorination rates in groundwater increased to a level sufficient to reduce contaminant flux to the vadose zone.

## 5.5 RESULTS PHASE 2 AND 3: ZVI

Analysis of the ZVI treatment results is presented in Truex 2011 and summarized below. Seasonal water table variation occurred over this test timeframe and the water level decreased such that the test cell screens were below 90% saturated after day 121 with increasing water levels starting around day 184. For this reason, the mass-discharge analysis focused on the first 120 days of treatment, 60 days under ambient conditions (Phase 2), and 60 days of heated treatment (Phase 3).

### *Geochemical Response*

ZVI reactions in groundwater cause a decreased oxidation-reduction potential (ORP) and an increase in pH. The ORP substantially decreased in the test cell upon addition of ZVI and remained low, generally between -100 and -200 mV for the first 150 days of the test, spanning both ambient temperature and elevated temperature conditions. When the ORP initially increased it was an indication of the ZVI losing its ability to maintain chemically reducing conditions. The low ORP conditions were maintained longest at the injection well where the highest concentration of ZVI was present in the aquifer. Changes in pH (increased due to ZVI reactions with water) showed similar trends in terms of the timeframe of ZVI reactions at the monitoring locations.

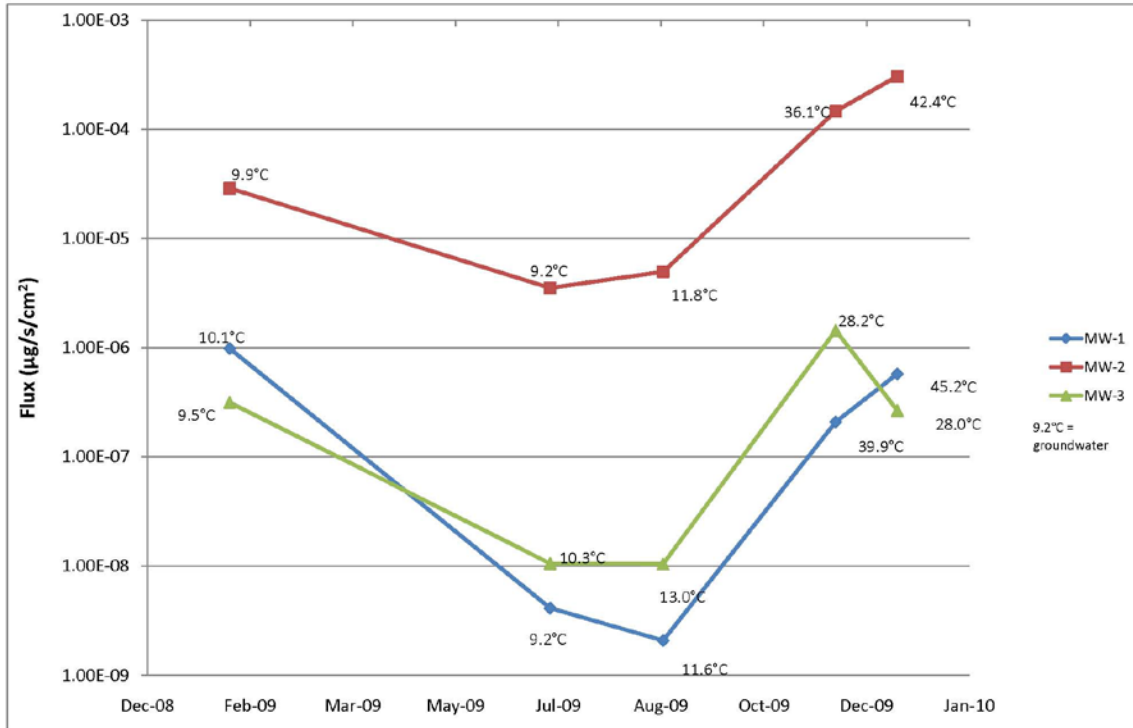


Figure 6. TCE vapor flux during Phase 1, 2 and 3 for ISB test cell.

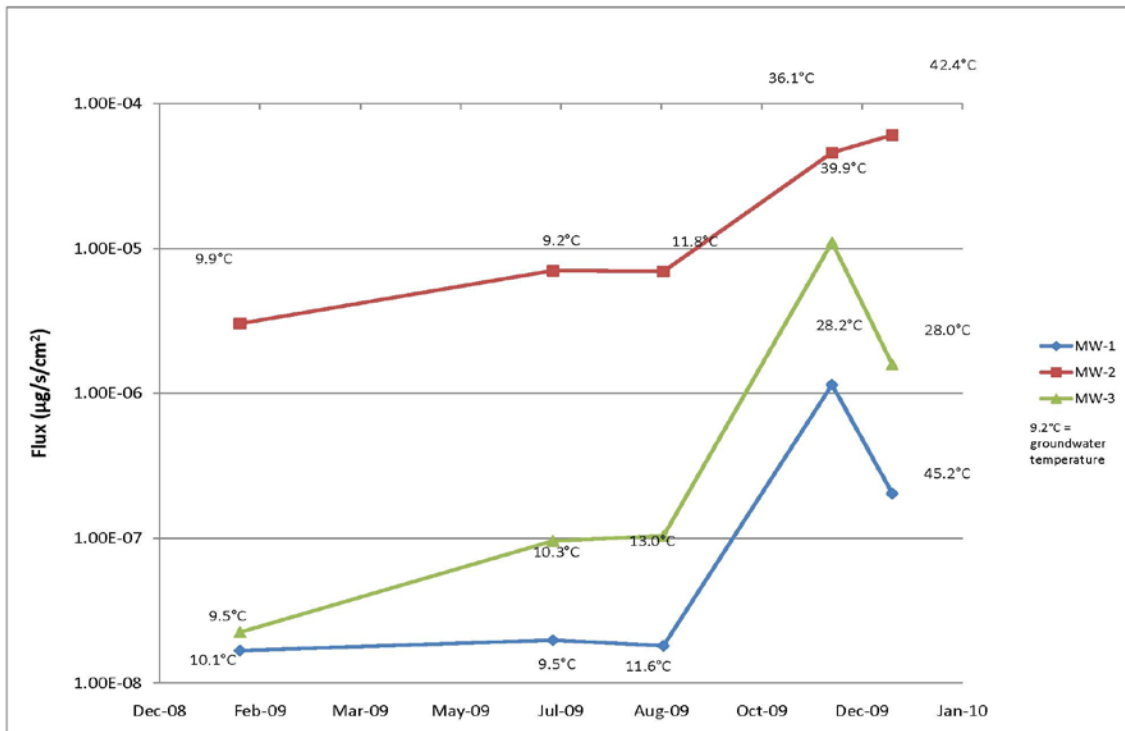
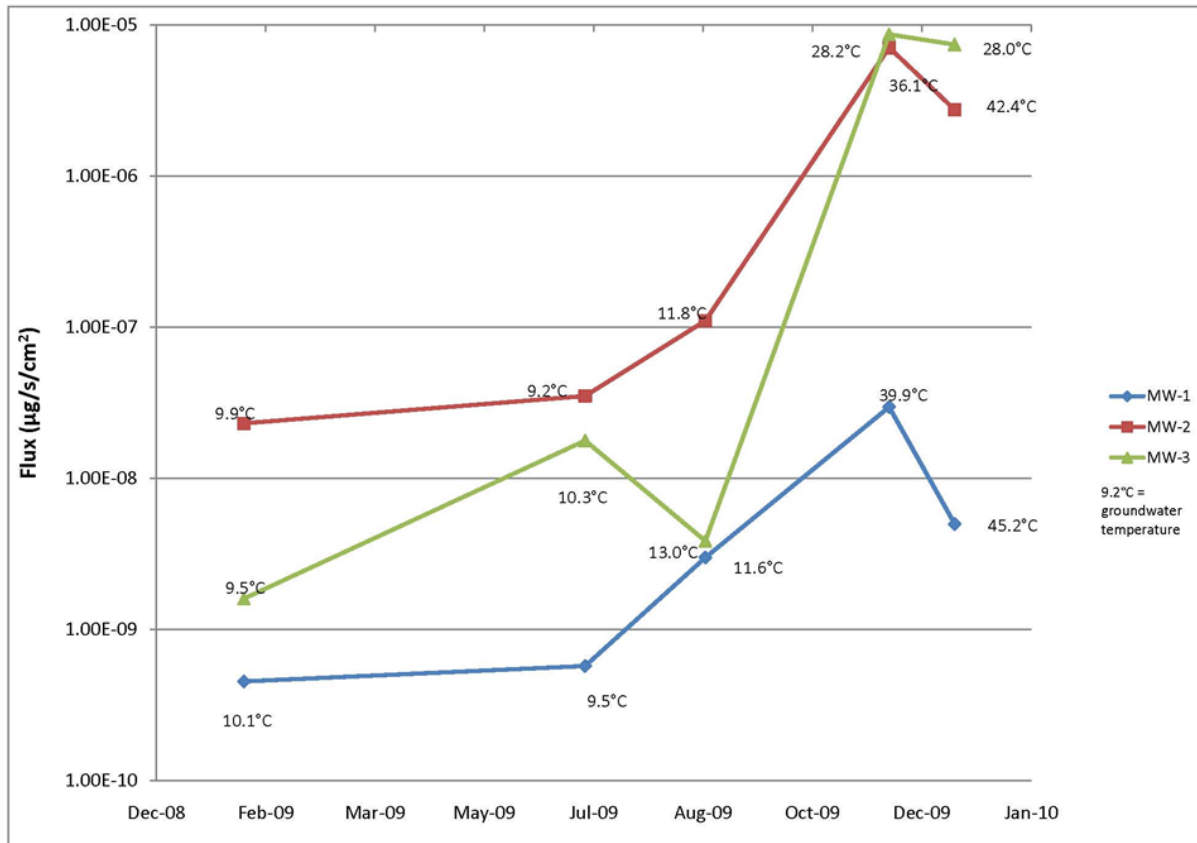


Figure 7. cis-DCE vapor flux during Phase 1, 2 and 3 for ISB test cell.



**Figure 8. VC Vapor Flux during Phase 1,2 and 3 for ISB Test Cell.**

### *Contaminant and Dechlorination Product Concentrations*

While most of the results interpretation requires a mass-discharge analysis (discussed in Section 6), some general conclusions about contaminant dechlorination can be drawn directly from the contaminant data and are presented below.

At all interior test cell wells, dechlorination daughter products appeared within one week of ZVI injection and showed primarily dechlorination products present between 44 -120 days after injection. Figure 9 illustrates the chloroethene response calculated. Charts illustrating the chloroethene response observed in each MW are presented in the Final ER-0719 Report (CDM Smith 2012). The total organic dechlorination products show a sharp increase during the first 60 days of heating, days 60 – 120 after injection, and then begin to decline. The dominant organic dechlorination daughter products observed were cis-1,2-DCE, ethene, and ethane, indicative of both beta elimination and reductive dechlorination mechanisms. The increases in cis-1,2-DCE concentrations suggest that incomplete biological dechlorination of TCE to cis-1,2-DCE was stimulated rapidly, potentially induced by hydrogen produced by the ZVI. With the absence of VC, the complete biological reductive dechlorination pathway is unlikely and the ethene and ethane concentration increases suggest that beta elimination dechlorination reactions catalyzed by the ZVI were occurring. Acetylene is a transient product of the abiotic reactions and was observed at concentrations ranging between 0.4uM - 1.2 uM.



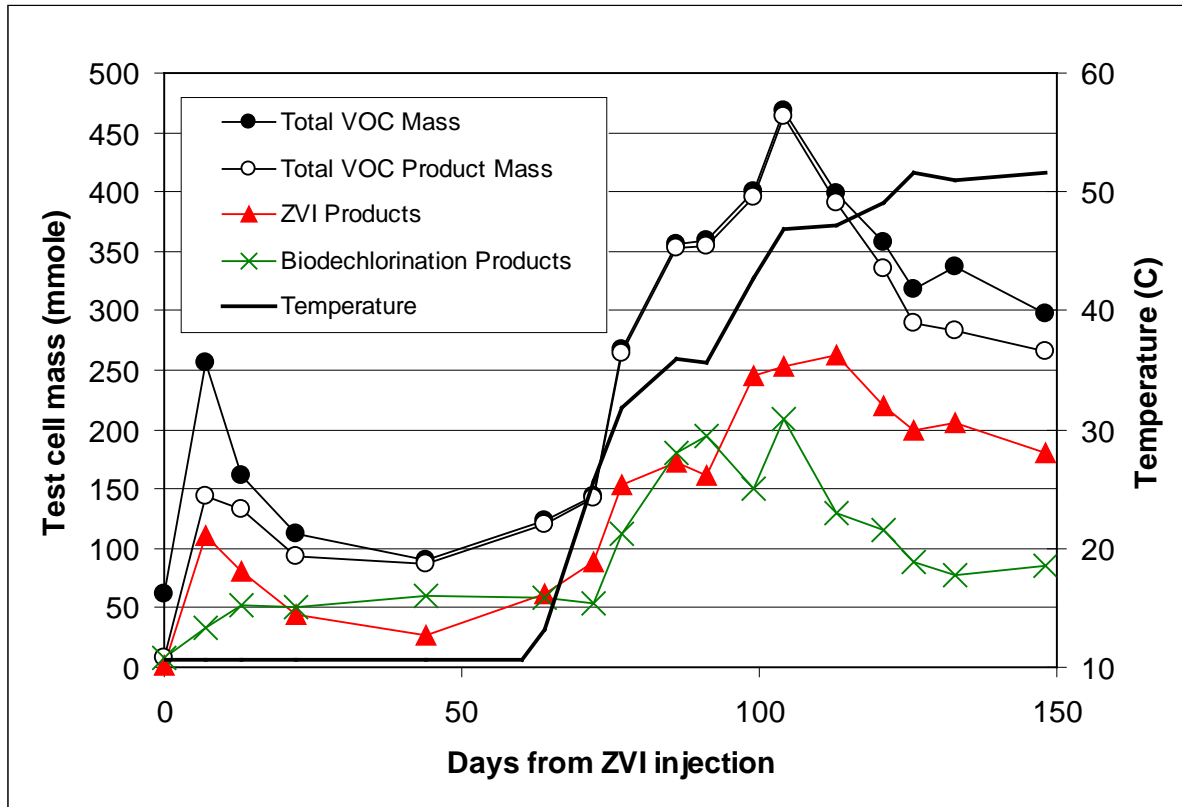


**Figure 9. Total VOC mass within the ZVI test cell.**

Increases in dechlorination products and decreases in TCE concentration with an overall increase in the total VOC concentration indicate that sediment- or NAPL-associated TCE was being treated and that the ZVI reaction transformed TCE at least as quickly as it was being released from the sediment, even under elevated temperature conditions. The groundwater data also indicate that the ZVI induced both reductive dechlorination and beta elimination reactions (Section 6). As an overall indication of treatment, Table 11 shows the TCE and dechlorination concentrations in the groundwater before ZVI injection and at the end of the test. Treatment during the full Phase 2 and 3 duration of the ZVI test resulted in a decrease in groundwater TCE concentration. Except for DCE, final groundwater concentrations of organic dechlorination products were 1 to 2 orders of magnitude higher at the end of treatment. Table 11 also shows that initial TCE concentrations were much higher inside compared to outside the test cell, indicating that the test was conducted in a contaminant source zone.

### ***Soil Vapor Monitoring***

Concentrations of TCE, DCE, VC, ethene, ethane, and acetylene were measured in soil gas samples collected from the unsaturated filter pack sand above the well screen intervals in ZVI-MW2 through –MW7. These data imposed a problem in quantifying volatilization from the groundwater, therefore were not used in the mass-discharge analysis presented in Section 6, but are presented in the Final ER-0179 Report (CDM Smith, 2012).

**Table 11. Average groundwater concentration of TCE and dechlorination products.**

	<b>TCE (ug/L)</b>	<b>DCE (ug/L)</b>	<b>VC (ug/L)</b>	<b>Ethane (ug/L)</b>	<b>Ethane (ug/L)</b>
<b>Test cell (INJ, MW1, MW2, MW4, MW5, MW6, MW7)</b>					
Start	3794	672	1	3	5
Finish	93	605	32	171	176
<b>Outside (MW9)</b>					
Start	49	17	0	0	0
Finish	37	64	0	0	0

### ***Soil Monitoring***

Soil concentrations of TCE, DCE, and VC were measured before ZVI treatment, at the end of Phase 2 ambient treatment, and at the end of the test after Phase 3 heated treatment. Figure 10 shows the TCE soil concentrations. DCE and VC soil concentrations were much lower than the TCE concentrations and are presented only in the Final ER-0179 Report (CDM Smith, 2012). By the end of the test, soil TCE concentrations were low at all locations dropping to below 1 milligrams per kilogram (mg/kg) at the injection well. These data suggest that significant treatment of TCE contaminant mass occurred during the test. Other test data suggest that substantial TCE mass reduction occurred by day 120 of the treatment. The amount of mass reduction due to volatilization rather than reaction is difficult to quantify due to the lower data density after day 150. However, in all of these data, the TCE groundwater concentrations were lower than the concentrations of dechlorination products, suggesting that volatilization of TCE was low compared to dissolution and reaction.

## **5.6 PHASE 3: LOW-ENERGY ERH**

### ***Power and Energy***

During Phase 3 of operations, energy input for the ZVI and ISB test cells were 60,038 kWh and 33,330 kWh respectively; totaling 93,368 kWh for the entire project. Figure 11 summarize the total cumulative energy input to both the ZVI and ISB test cells. During initial heat up of the ZVI test cell daily power application rates averaged 30 kilowatt (kW) with weekly energy application peaking at 4,333 kWh during week three of operations. During initial heat up of the ISB test cell daily power application rates averaged 35-40 kW with weekly energy application peaking at 3,775 kWh during week two of operations. ERH temperatures averages and power usage is detailed in the Final ER-0179 Report (CDM Smith, 2012).

### ***Temperature***

Heating of the ZVI and ISB test cells was initiated at the beginning of Phase 3 until the desired temperature range (40-50°C), and (30-40°C) respectively was reached. Average temperatures within, upgradient and downgradient of the ZVI test cell are shown in Figure 12 and within the ISB test cell are shown in Figure 13.

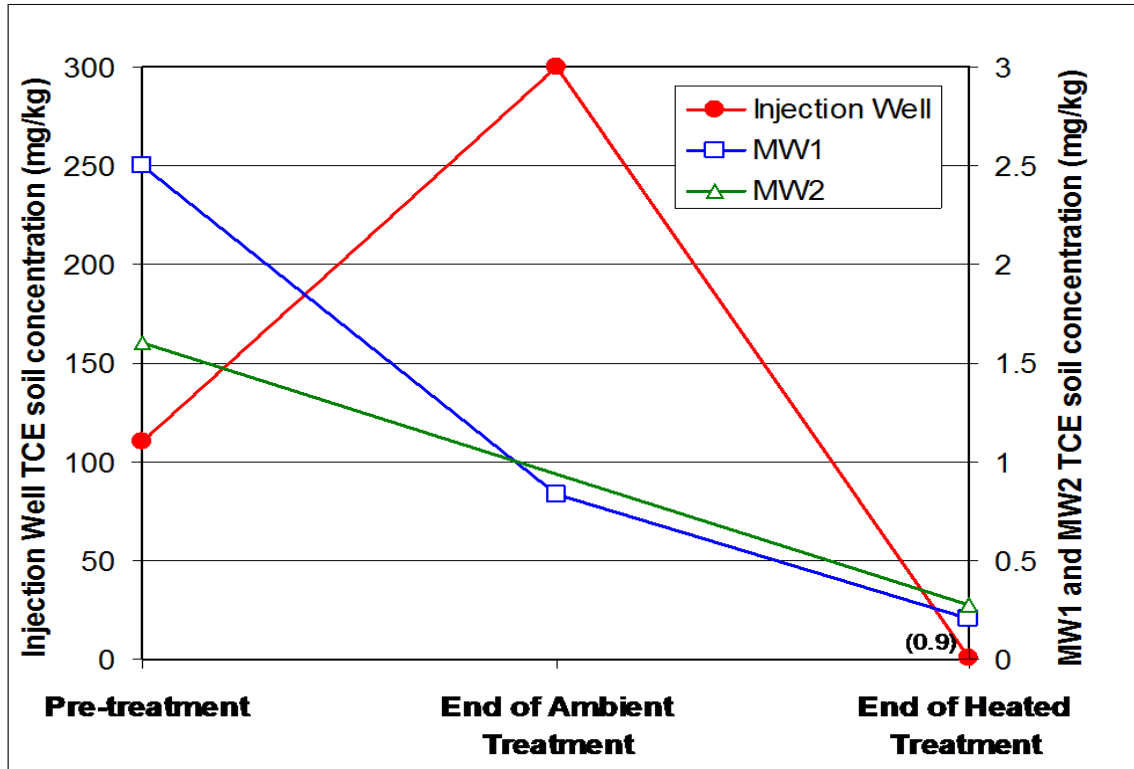


Figure 10. Soil concentrations of TCE, DCE, and VC measured before ZVI treatment Nd at the end of Phase 2 and Phase 3.

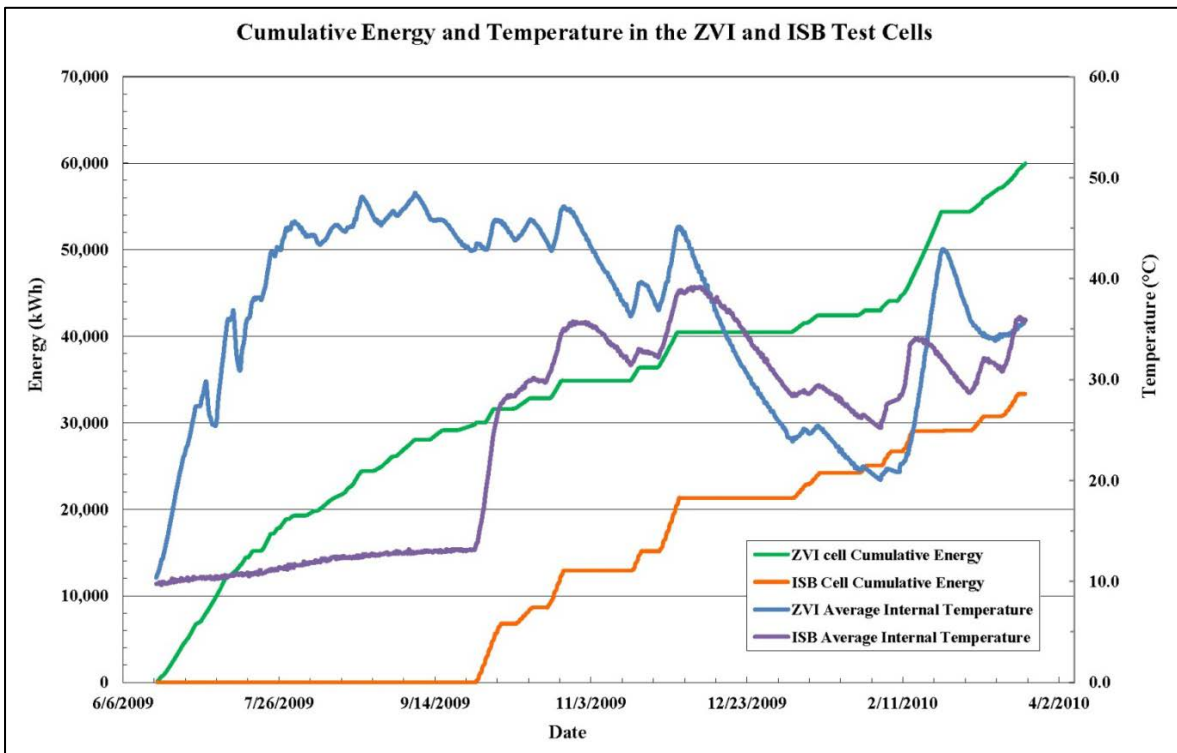


Figure 11. Cumulative energy and temperature in ZVI and ISB test cells.

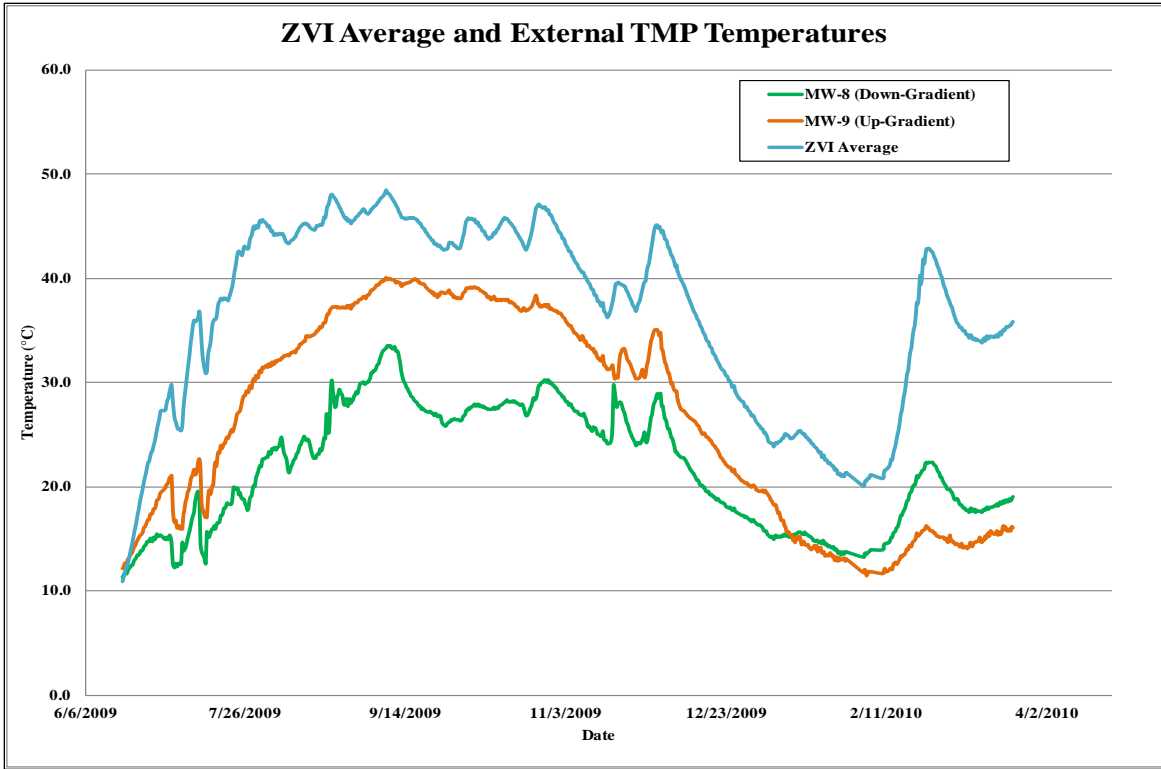


Figure 12. Average external ZVI test cell TMP temperatures.

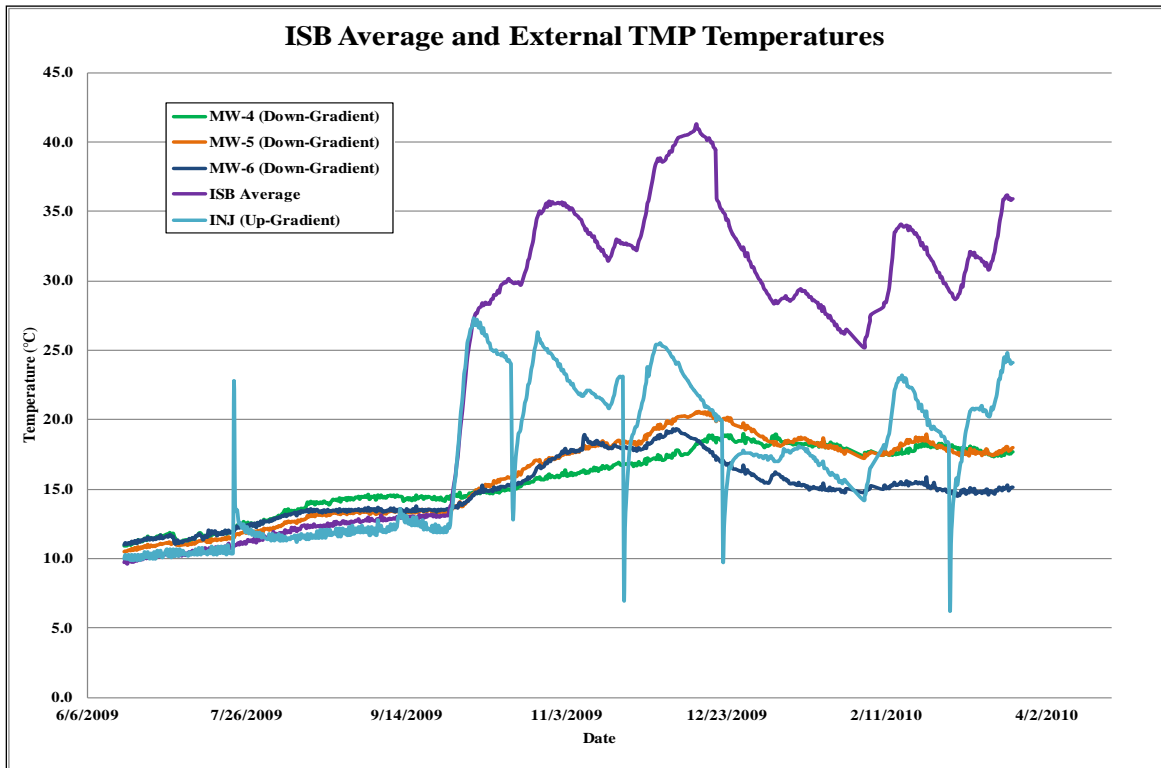


Figure 13. Average external ISB test cell TMP temperatures.

*This page left blank intentionally.*

## 6.0 PERFORMANCE ASSESSMENT

Performance of the demonstration project was evaluated by conducting a mass balance assessment using a mass discharge approach in the test cells. However, how the approach applied varied due to the system configurations and results of each of the ISB and ZVI demonstrations. A mass discharge analysis was developed and applied to quantify the treatment zone processes using the data from MWs and considering the rate of groundwater flow through the treatment zone (e.g., Figure 14). The mass discharge analysis computes rates of the multiple processes in the treatment zone by comparing the inflow and outflow discharge rates for either the entire test cell (as for the ISB demonstration) or for a defined segments for the ZVI test cell. Because the treatment zone is a contaminant source area and upgradient water is relatively uncontaminated, dissolution from DNAPL or sediment-associated TCE is the main mechanism adding contamination to groundwater. Treatment performance in terms of reducing the contaminant source is a function of the relative rates of 1) contaminant dissolution to the groundwater, 2) migration out of the treatment zone due to advection or volatilization, and 3) contaminant degradation. In the field, constituent concentrations from MWs are the primary data available to quantify these processes.

The first step of the analysis was to compute the influent and effluent discharges from either the ISB test cell or the ZVI test cell segments. For the analysis, mass is represented as moles so that stoichiometric relations of different groundwater constituents can be considered. The influent mass discharge of constituents was estimated from Equation 1.

$$MD_{in} [mmol \cdot d^{-1}] = C_{upgradient} Q \quad (\text{Equation 1})$$

The effluent mass discharge in the water phase was estimated from Equation 2.

$$MD_{out-w} [mmol \cdot d^{-1}] = C_w Q \quad (\text{Equation 2})$$

The net contaminant dissolution rate  $N_d$  was estimated using Equation 3.

$$MD_{Dissolution} = (MD_{out-w} + MD_{out-v})_{TCE+products} - MD_{in-TCE+products} \quad (\text{Equation 3})$$

The net TCE dissolution rate  $N_d$  was estimated using Equation 4.

$$N_d = (MD_{out-w} + MD_{out-v})_{TCE} - MD_{in-TCE} \quad (\text{Equation 4})$$

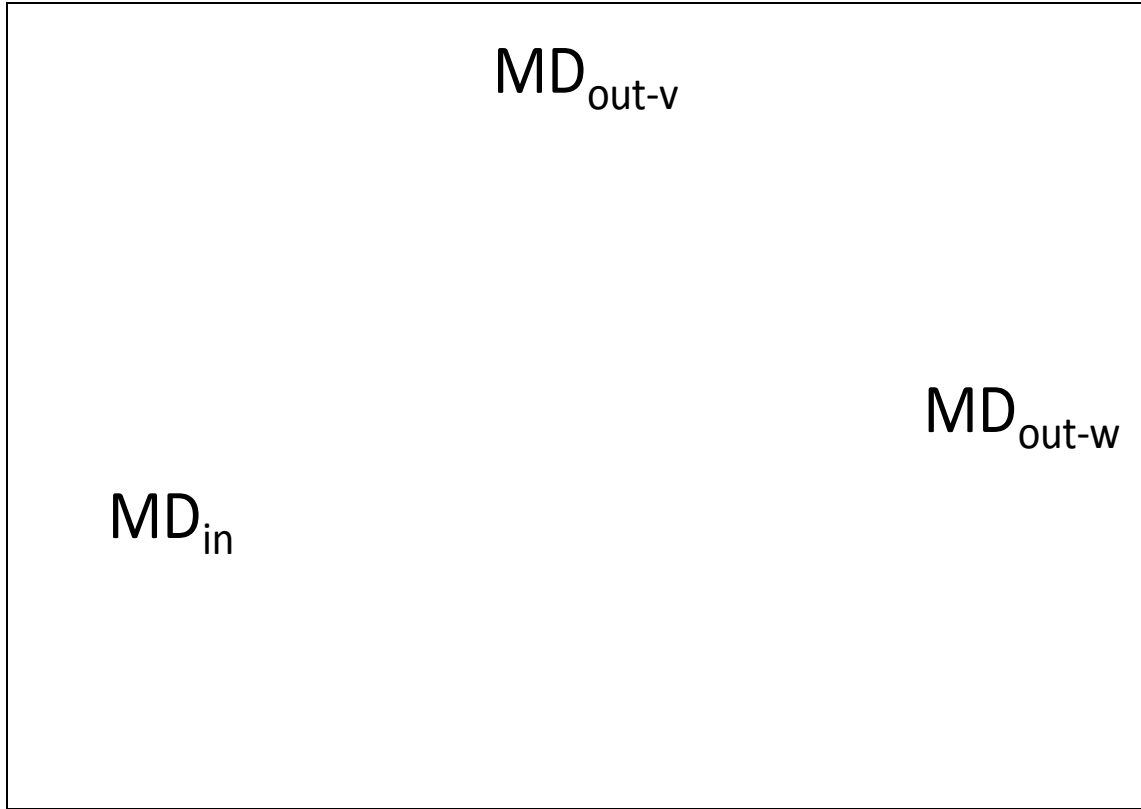


**Figure 14. Mass-discharge analysis configuration where  $MD_{in}$  is the influent mass discharge and  $MD_{out-w}$  and  $MD_{out-v}$  are the effluent mass discharge in the water and vapor phases, respectively.**

Dechlorination reaction rates,  $R$  (mmol d-1), were estimated using two methods, evaluating reductive daughter product concentrations using Equation 5 and evaluating chloride data using Equation 6.

$$R = (MD_{out-w} + MD_{out-v})_{products} - MD_{in-products} \quad (\text{Equation 5})$$

$$R_{tc} = MD_{out-w-chloride} - MD_{in-chloride} \quad (\text{Equation 6})$$

With respect to the processes shown in Figure 14, sorption of dechlorination products to sediments is low at the site (Truex 2006) and was not included in the analysis. Initial sediment concentrations of DCE were one to two orders of magnitude lower than TCE sediment concentrations and VC, ethene, and ethane were not detected. Thus, dissolution of TCE as a contamination source was the only dissolution process included in the analysis. The specifics of how these concepts were applied for each of the ISB and ZVI test cells is provided below.

## 6.1 MASS BALANCE FACTORS ISB

### 6.1.1 ISB Enhanced Mass Transfer

A mass balance evaluation of the ISB test cell was conducted to quantify changes in 1) contaminant dissolution from the residual contaminant mass to groundwater, 2) migration out of the treatment zone due to advection or volatilization, and 3) contaminant degradation using the mass discharge approach. Conceptually, the approach was to quantify a mass balance as shown in Figure 14 and Equations 1-4.

Contaminant concentrations outside the ISB heated zone were 2-4 orders of magnitude lower than within the test cell. Therefore, it was assumed that mass discharge into the test cell ( $MD_{in}$ ) was negligible. In addition, the total mass discharge based on Figure 14 and Equations 3 and 4 also account for mass leaving the test cell in soil gas. Table 12 presents the total mass discharge in the groundwater ( $MD_{out-w}$ ) across the ISB-MW2 and -MW1 transect and in soil gas across the entire heated zone area ( $MD_{out-v}$ ) for two timepoints in Phase 2 and two in Phase 3. As shown, the contribution of  $MD_{out-v}$  represented by soil gas in both Phase 2 and Phase 3 ranged from 0.02-1.45% of the total. Therefore, the contaminant mass discharge modeled using MVS across transect ISB-MW1 and ISB-MW2 was used to evaluate enhanced dissolution ( $MD_{dissolution}$ ) and reaction kinetics, and  $MD_{out}$  represented by soil gas was negligible and not included in the analysis.

Hydraulic conductivity data and groundwater elevation data were used to calculate mass flux and mass discharge. The average horizontal hydraulic conductivity measured at ISB-MW1 and ISB-MW2 for each of three depth intervals (approximately 12, 17 and 22 ft bgs) was used (Table 5). The vertical hydraulic conductivity was set at half the magnitude of the horizontal hydraulic conductivity. Groundwater elevation and contaminant concentrations measured at each timepoint were then input into the model and kriged in three dimensions. Groundwater contaminant mass flux was then calculated in three dimensions and a transect set through ISB-MW2 and -MW1 was used to evaluate mass discharge by integrating the mass flux values over the transect area (approximately 16 ft wide by 21 ft deep). This was used to develop the estimates for  $MD_{out}$  for total VOCs (TCE + products), reductive daughter products (DCE, VC, ethene) and chloride.

The total VOCs dissolution rate ( $MD_{dissolution}$ ), reaction rate using daughter products (R) and reaction rates using chloride ( $R_{tc}$ ) over the course of the demonstration was plotted as a function of temperature (Figure 15). These data indicate a positive correlation for  $MD_{dissolution}$  ( $R^2 = 0.53$ ), R ( $R^2=0.45$ ) and  $R_{tc}$  ( $R^2=0.60$ ) as a function of temperature from the test cell.

The  $MD_{dissolution}$  due to heating in Phase 3 was evaluated by comparing  $MD_{out}$  of total VOCs as a function of temperature. For this analysis, the influent  $MD_{in}$  and vapor  $MD_{in-vapor}$  were assumed negligible. Based on the correlation in Figure 15, the total VOC dissolution increases by a factor of 4.6, or an increase from 177 g VOC as TCE/d to 812 g VOC as TCE/d when temperatures are increased from 10°C to 40°C. The increase is largely attributed to enhanced mass transfer due to the elevated temperature as opposed to reductive dechlorination reactions (i.e., enhancing the concentration gradient due to removal parent compounds and formation of daughter products) because the comparison was made between Phase 2, where dechlorination reactions had already been established at ambient temperatures and Phase 3. This is in good



**Table 12. Comparison of mass discharge from the ISB test cell in groundwater and in soil gas.**

Date	Days	Phase	Vapor Discharge <sup>a</sup> (MD <sub>out-v</sub> )			Groundwater Discharge (MD <sub>out-w</sub> )			Total Discharge		
			TCE (g/d)	cDCE (g/d)	VC (g/d)	TCE	cDCE	VC	TCE	cDCE	VC
July 2, 2009	147	2	0.03	0.06	0.00	29.72	297.91	1.32	29.75	297.97	1.32
August 26, 2009	193	2	0.04	0.06	0.00	11.99	102.48	0.80	12.04	102.54	0.80
November 18, 2009	286	3	1.25	0.49	0.13	86.54	271.37	21.03	87.79	271.86	21.17
December 18, 2009	314	3	2.58	0.52	0.09	252.13	398.53	31.71	254.71	399.06	31.79

<sup>a</sup>Average vapor flux calculated by averaging flux for MW1, MW2, MW3 and multiplying by test cell area.

agreement with Imhoff 1997, which described the enhanced dissolution of TCE DNAPLs during hot water flushing. In this work the aqueous phase mass transfer coefficient,  $K_a$ , was developed experimentally and results applied to the empirical model. Increasing temperatures from 10°C to 35°C increased in  $K_a$  by a factor of 2 and by 3 when temperatures increased to 55°C. These data suggest that significant enhanced dissolution occurs within areas containing DNAPLs at elevated temperatures.

### 6.1.2 ISB Impact of Elevated Temperature on Kinetics

To evaluate the impact of heating on treatment rates of TCE, the rate ( $R$ ) was evaluated using Equations 4 and 5. First the reaction rate was estimated using reductive daughter products where  $MD_{out}$  of reductive daughter products was evaluated and used as the reaction rate,  $R$  (mmol/d). For this analysis, the influent  $MD_{in}$  and vapor  $MD_{in-vapor}$  were assumed negligible. Based on the correlation developed in Figure 15, the  $R$  estimated increased by a factor of 3.6 when you increase temperatures from 10°C to 40°C or increase from 175g TCE treated/day to 585 g TCE treated/d.

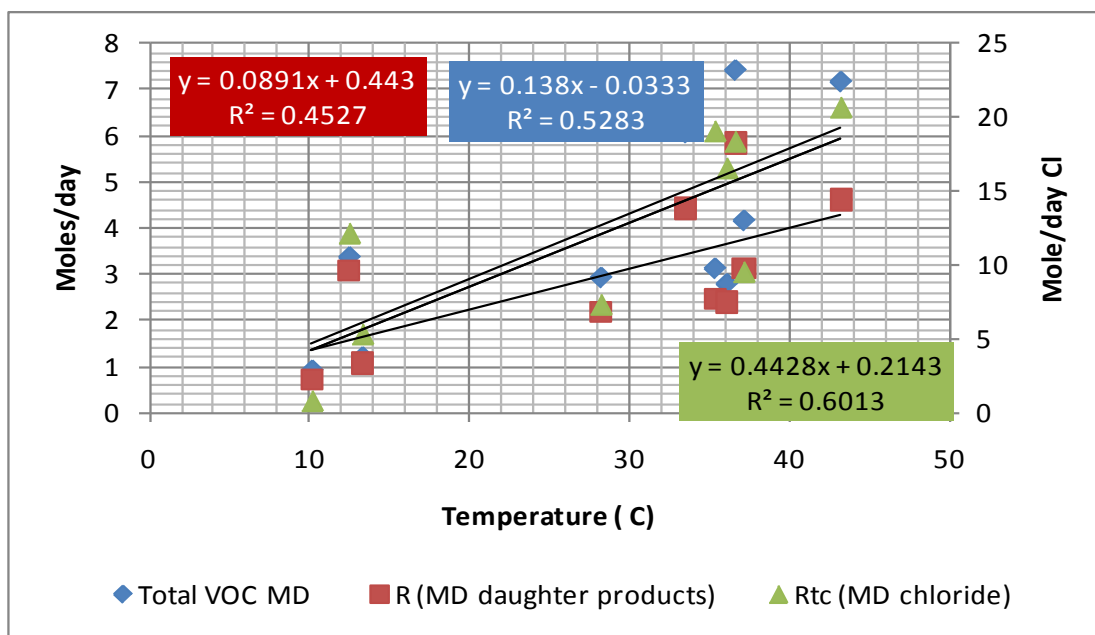


**Figure 15. Linear correlation between MDdissolution,  $R$ , and  $R_{tc}$  as a function of temperature.**

Similarly, the rate of mass discharge of treated TCE can also be evaluated using chloride and Equation 5. The  $R_{tc}$  estimated using  $(MD_{out})_{chloride}$  increased by a factor of 5.3 when you increase temperatures from 10°C to 40°C which corresponded to an increase from 337 to 1789 g TCE treated/d. The difference in these values is likely due to that fact that chloride is more conserved than the reductive daughter products especially compared to VC and ethene, which are lost to volatilization and biological oxidation. These are generally in good agreement with the Arrhenius equation, which suggests that the rate of reaction generally doubles for every 10°C increase in temperature; this would correspond to a factor of 8 increase in rate of reaction at 40°C compared to 10°C. However, a direct assessment of kinetics cannot be established due to

the increased flux of contaminants dissolved from the residual phase. The reaction rate  $R$  and  $R_{tc}$  is the total reaction rate resulting from both enhanced mass transfer and dechlorination reactions.

In order to assess the relative significance of enhanced mass transfer and dechlorination reactions an evaluation was conducted to quantify the relative mass discharge rates of TCE compared to total VOCs and reductive daughter products. An objective of the demonstration was to ensure that in situ dechlorination could treat TCE dissolved from the residual phase due to elevated temperatures and account for losses due to from volatilization or dissolution and advection. Therefore, mass discharge analysis included quantification the amount of TCE released from sediment- or NAPL-associated TCE ( $N_d$  from Equation 4) into the groundwater compared to the rate of the ISB reactions to transform the TCE. The proportion of  $N_d$  following Phase 2 activities that TCE represented was approximately 12 g TCE/d of the 625 g total VOC as TCE/d (accounting for approximately 2% of the total contaminant mass discharge). This suggests that the transformation rate was fast enough to dechlorinate TCE to reductive daughter products at the ISB-MW1 and MW-2 boundary.

During heating (Phase 3), the TCE mass discharge,  $N_d$ , increased reaching a maximum in December (day 314) with 252 g TCE /d of the total 943 g VOC as TCE/d (accounting for approximately 27% of the mass). This indicates that at the ISB-MW1 and-MW2 boundary that TCE was being discharged, although treatment rates were degrading nearly 75% of the mass. However, the ISB-MW1 and -MW2 boundary was within the DNAPL zone, especially at ISB-MW2. Therefore, the analysis was expanded to evaluate contaminant flux to areas downgradient of the test cell. The ISB treatment area was much larger than the heated treatment zone due to transport of carbon downgradient of the test cell. Transport of TCE and reductive daughter products was evaluated in three downgradient MWs ISB-MW4, -MW5 and -MW6. Of these, ISB-MW4 was the most impacted location due to its proximity downgradient of ISB-MW2. Following the onset of heating, an initial slug of DCE was observed at this location, with very low TCE concentrations (see Figure 7). During the December, 2009 (day 314) and January, 2009 (day 355) sampling events, the TCE (93 and 20  $\mu\text{g/L}$ ), DCE (65 and 340  $\mu\text{g/L}$ ) were much lower than observed at ISB-MW2, suggesting attenuation was occurring along the flow path. In addition, the proportion of VC also dramatically increased with time. These data suggest that although TCE was mobilized, it could be mitigated, and treated, by creating a sufficiently large treatment area downgradient of the source zone to ensure treatment of mobilized TCE.

## **6.2 MASS BALANCE FACTORS ZVI**

### **6.2.1 ZVI Mass Transfer**

A mass balance/mass discharge analysis was applied to evaluate TCE dechlorination, dissolution, advection, and volatilization in the ZVI test cell. The analysis was designed to account for the ZVI distribution and hydraulic conditions in the test cell. Key considerations are described below.

ZVI mass in the test cell was highest surrounding the injection well (Truex 2010). The ZVI test cell was centered on a high TCE contamination zone surrounded by groundwater at much lower TCE concentrations. Additionally, ZVI was distributed to the test cell using SlurryPro™, a shear-thinning fluid, which when static has a high viscosity (Truex 2010). Data suggest that the

groundwater flow rate through the ZVI test cell was much slower than the flow rate prior to injection of the ZVI and SlurryPro™, with a nominal post-injection value based on tracer elution of 0.38 m/d (Truex 2010, 2011). While the flow rate could not be evaluated over the course of the test; test data do not suggest a large change in flow rate during the test. If a change were to occur, it would have increased the flow rate over time as the viscosity of the SlurryPro™ decreased due to dispersal or degradation. Thus, comparison of rates between initial Phase 2 ambient temperature operation and Phase 3 heated operations would tend to be conservative and underestimate rates in Phase 3 versus Phase 2 if the groundwater flow rate increased over time.

Based on the above considerations, the mass discharge (moles per time) was estimated for assigned test cell segments through well INJ as shown on Figure 14. The mass discharge analysis was applied to evaluate dechlorination in this segment along a flow path through the center of the test cell. This segments fall along the nominal flow path of groundwater through the test cell that intersects the zone of highest ZVI concentration (i.e., surrounding the injection well). The longitudinal dimension of the segment was based on the estimated distance to the edge of the ZVI/SlurryPro™ injection. The segment used a unit lateral dimension of 1 m and a thickness equal to the well screen interval (1.5 m).

The mass discharge analysis is presented in Truex 2011 and repeated here. A mass-discharge analysis was developed and applied to quantify the treatment zone processes using the data from MWs and considering the rate of groundwater flow through the treatment zone segments ending at each MW (Figure 16). The mass-discharge analysis computes rates of the multiple processes in the treatment zone by comparing the inflow and outflow discharge rates for a defined segment as shown in Figure 16. Because the treatment zone is a contaminant source area and upgradient water is relatively uncontaminated, dissolution from DNAPL or sediment-associated TCE is the main mechanism adding contamination to groundwater. Treatment performance in terms of reducing the contaminant source is a function of the relative rates of 1) contaminant dissolution to the groundwater, 2) contaminant degradation, and 3) migration out of the treatment zone due to advection or volatilization. In the field, constituent concentrations from MWs are the primary data available to quantify these processes. Additionally, a source area treatment analysis is unlike an analysis for a permeable reactive barrier where the primary goal is reduction of upgradient contaminants as they flow through the treatment zone.

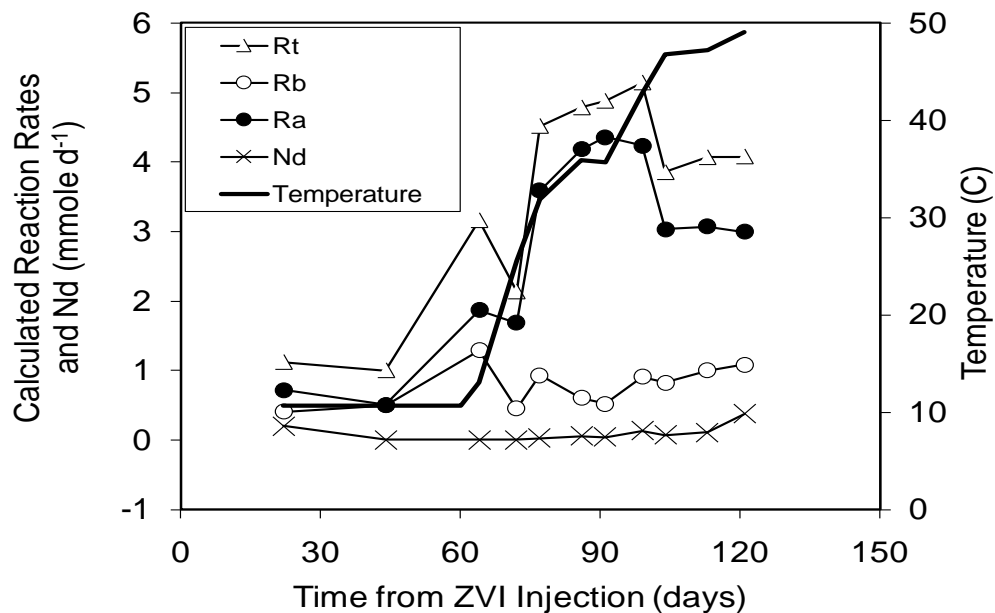


**Figure 16. Calculated TCE reaction rates and Nd for the INJ segment.**

The first step of the analysis was to compute the influent and effluent discharges of the segments. For the analysis, mass is represented as moles so that stoichiometric relations of different groundwater constituents can be considered. The influent mass discharge of constituents to each segment was estimated from Equation 1 where  $C_{\text{upgradient}}$  [mmol L<sup>-1</sup>] is the concentration at well ZVI-MW9. Data for well ZVI-MW9 was assumed to represent conditions upgradient of the test cell because the ZVI injection did not reach this well (Truex 2010). A groundwater flow rate,  $Q$ , of 103 L/d was calculated from the estimated linear velocity, porosity (0.18), and cross section area of the segments using Darcy's Law and assumed to remain constant. The effluent mass discharge in the water phase was estimated from Equation 2 where  $C_w$  [mmol/L] is the concentration at the MWs for the selected segments.

The effluent mass discharge in the vapor phase was estimated from Equation 6.

$$MD_{\text{out-v}} [\text{mmol} \cdot \text{d}^{-1}] = D_{\text{as}} A_v \left( \frac{C_w H}{L_v} \right) \quad (\text{Equation 6})$$

The diffusion coefficient for each compound in sediment,  $D_{\text{as}}$ , was calculated from the individual gas diffusion coefficients (Yaws, 2003) ( $T=25^\circ\text{C}$ ) using the method of Millington and Quirk (1961), the measured porosity, and moisture content (14.5% [v/v]). The dimensionless Henry's Law coefficient,  $H$ , corrected for temperature was calculated for each compound from tabulated vapor pressure (Yaws 2009) and solubility data (Yaws, 2009; Mackay, 2006) as a function of temperature. The distance from the water table to the ground surface,  $L_v$ , was estimated as the average vadose zone thickness of 2.13 m. The surface area for diffusive mass transfer,  $A_v$ , was based on the distance from the upgradient edge of the treatment zone to the MW with a unit width of 1 m. Soil gas data were not used in the analysis because pre-test vapor-phase TCE and DCE concentrations were an average of 69 and 15 times higher, respectively, in

samples from the unsaturated sand pack of wells ZVI-MW2 through -MW7 than vapor concentrations calculated based on the measured groundwater concentration and equilibrium partitioning by Henry's Law. These data indicated the presence of significant vadose zone contamination that would interfere with directly measuring volatilization of TCE and DCE from the groundwater.

The next phase of the analysis relates the segment inflow and outflow of groundwater constituents, computed using Equations 1-3, to the rates of reactions and processes occurring in these segments. This approach enables estimation of the overall TCE dissolution and degradation rates, the amount of TCE released from the source but untreated, and the reaction rates producing specific reaction products as a function of the conditions within the test cell (e.g., temperature). These segment reaction rates define the treatment performance and, along with the ZVI amendment information, can be used for process scale-up and performance estimation.

When all organic dechlorination products were considered, the estimated reaction rate from Equation 4 represents the overall rate of TCE transformation,  $R_t$ . An abiotic reaction rate,  $R_a$  (elimination reaction), was estimated using Equation 4 by only considering transformation to ethene, ethane, and acetylene products. A biotic reaction rate,  $R_b$ , was estimated using Equation 4 by only considering transformation to DCE as the product, representing the combined effect of both biotic and direct ZVI hydrogenolysis reactions. Because negligible VC was observed during the test (3 to 4 orders of magnitude lower concentrations than DCE), it was assumed that biological dechlorination converted TCE to DCE only. One could consider  $R_a$  as representing the sum of reactions that produce non-hazardous products and  $R_b$  as DCE-producing reactions. The actual reactions occurring in the treatment zone are likely a mix of biotic and abiotic reactions. For instance, ZVI degrades DCE and VC, though at lower rates than TCE. Additionally, some biotic dechlorination beyond DCE is possible, though unlikely due to low observed VC concentrations. Molecular deoxyribonucleic acid (DNA) data targeting *Dehalococcoides*, the bacteria that converts cis-DCE to ethene, remained at low levels during the test, generally below the threshold concentration of  $10^6$  gene copy/ L to observe significant complete biotic dechlorination at JBLM groundwater (Macbeth and Sorenson, ESTCP ER-0318 Final Report), indicating biotic cis-DCE dechlorination was limited (Truex, 2011).

The overall rate of TCE dechlorination was also estimated using chloride data,  $R_{tc}$  (mmol d<sup>-1</sup>), using Equation 5. To convert chloride data to the equivalent moles of TCE, the chloride stoichiometry can be assigned based on the relative molar amounts of DCE, ethene, and ethane products observed at each time point.

### 6.2.2 ZVI Kinetic Changes

The impact of temperature on the in situ dechlorination reactions induced by injected ZVI are reported in Truex et al. (2011) and detailed here. A mass discharge analysis was used to evaluate the performance of the treatment with respect to dechlorination as a function of temperature. Due to seasonal variation, the water level declined such that a portion of the screen was unsaturated starting at about day 121 reaching a minimum of 70% saturated thickness by day 184. Because of this large change in hydrologic conditions, and the fact that the majority of TCE residual mass in the ZVI test cell was largely at the water table, the dechlorination rate analysis was constrained to data over the first 121 days of treatment.

Figure 16 shows the calculated TCE dechlorination rates and released but untreated TCE (Nd) over the first 121 days for the INJ segment. Flow paths through the test cell are uncertain. However, the INJ segment represents flow from upgradient through the zone of highest ZVI concentration.

Abiotic reactions predominate in the INJ segment. For the INJ segment, overall TCE transformation,  $R_t$  was 3.6-4.8 times higher at temperatures above 30°C compared to rates at the ambient temperature (~10°C). This result is consistent with laboratory tests where the TCE degradation rate at 40°C was 2.5 to 3 times greater than the rate at 20°C in batch microcosms with ZVI, JBLM sediment, and groundwater (Section 5.3). The Nd remained near zero in the INJ segment through 121 days, suggesting that the overall *in situ* transformation rate was comparable to the gross TCE dissolution rate.

Chloride concentrations (Figure 17) were also used in a mass discharge analysis to estimate the dechlorination rate as a function of temperature. The chloride data show an increase of about an order of magnitude in concentration coincident with the increase observed for organic dechlorination products during heating for wells ZVI-INJ, ZVI-MW4, and ZVI-MW5. A 2-3 times increase in chloride was observed for wells ZVI-MW1 and ZVI-MW6 where moderate amounts of ZVI were delivered during injection (Truex et al., 2010) and moderate dechlorination rates based on organic products were observed. Chloride concentrations were generally declining by 120 days after ZVI injection, although chloride concentrations remain highest at wells ZVI-INJ and ZVI-MW4. Wells ZVI-MW2 and ZVI-MW7 show only small changes in chloride concentration during the test corresponding to the relatively small amount of ZVI delivered to these portions of the test cell (Truex, 2010) and low dechlorination rates based on organic products.

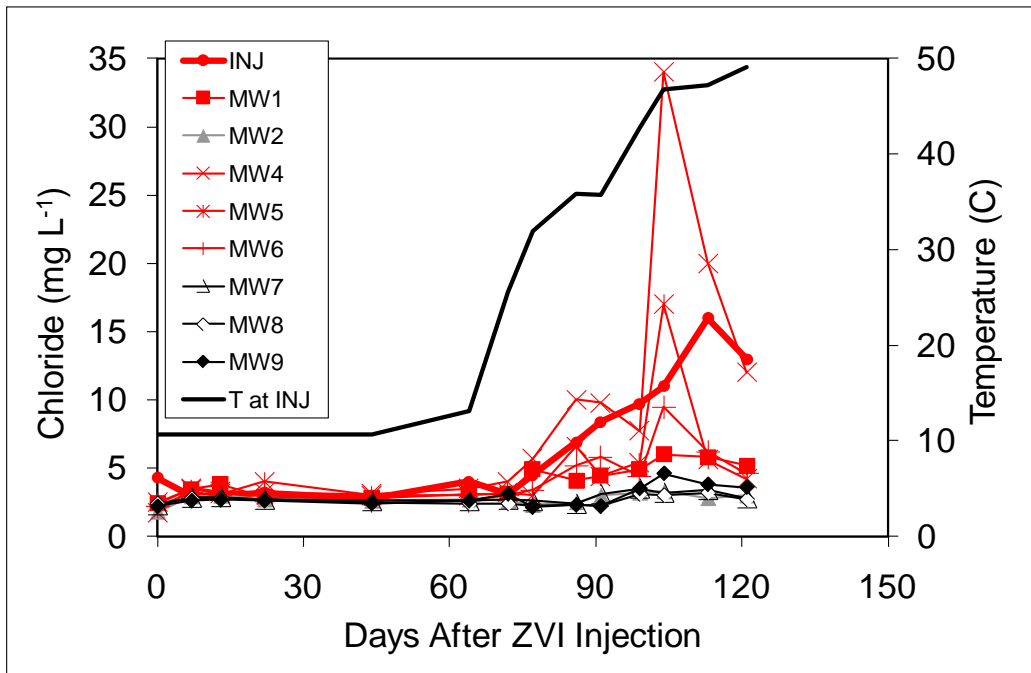


Figure 17. Chloride concentration over time in the ZVI test cell.

Average overall TCE transformation rates at the ambient temperature (~10°C) and for data at temperatures above 30°C through day 121 were calculated for the INJ segment using the organic dechlorination products ( $R_t$ ) and chloride ( $R_{tc}$ ) (Table 13). The two types of data show an increase in the reaction rate for temperatures above 30°C compared to the rate at the ambient temperature (~10°C). These and other field test data show that increasing temperature increases contaminant dissolution and degradation rates with minimal TCE volatilization and suggest that ZVI-based treatments can be enhanced with moderate heating. The mass discharge analysis provides a means to quantify the different processes occurring during treatment using MW data that is typically available for field applications.

**Table 13. Average overall rate of TCE transformation based on organic dechlorination products ( $R_t$ ) and chloride concentrations ( $R_{tc}$ ) (Truex et al., 2011).**

	$R_t$ [mmol-TCE d <sup>-1</sup> ]	$R_{tc}$ [mmol-TCE d <sup>-1</sup> ]
<b>Injection Well Segment</b>		
a) Ambient temperature	1.1	1.2
b) Temperature >30°C	4.6	9.7
Ratio (b/a)	4.4	8.3

### 6.2.3 Biotic/Abiotic

Overall, abiotic reactions dominated in the upgradient half of the test cell (ZVI-MW1, ZVI-MW2, ZVI-MW7, and ZVI-INJ) with biotic (hydrogenolysis) reactions becoming more prevalent toward the downgradient portion (ZVI-MW4, ZVI-MW5, and ZVI-MW6) (TCE reaction rates and Nd are presented for all wells in Truex et al., 2011).

### 6.2.4 Impact of Temperature on Dissolution/Volatilization

Analysis for the impact of temperature on dissolution and volatilization are presented in Truex et al. (2011) and repeated here. An objective of the combined process was to promote in situ dechlorination and minimize volatilization of TCE. The maximum calculated volatilization rate of TCE ( $MD_{out-v}$ ) at INJ (Equation 3) for the elevated temperature portion of the test (day 60 through 121) was about 1% of the  $R_t$  (Equation 4) due to the low aqueous TCE concentrations. By integrating the mass discharge from the INJ segment over the 121 day analysis period and assuming dechlorination was for sediment-associated TCE, the ZVI treatment reduced the average sediment concentration by 9 mg/kg in these segments with about 85% of this reduction occurring during the 60 days of heating.

The mass discharge analysis included quantification of the net TCE dissolution rate, Nd, as a means to evaluate the amount of TCE released from sediment- or NAPL-associated TCE into the groundwater in excess of the capacity of the ZVI reactions to transform the TCE (see Equation 5, Section 6.1.1). The Nd remained near zero in the INJ segments through 121 days, suggesting that the in situ degradation rate was comparable to the gross TCE dissolution rate over this time period (Figure 16) (Truex 2011). The TCE concentration in the test cell began to increase after about day 100. Thus, past day 120, while not specifically quantified as described above, the net TCE dissolution increased. Note, however, that the TCE concentrations do not rebound significantly at the injection well where the initial TCE concentration was dramatically higher



than elsewhere (e.g., indicative of the primary source zone). Higher ZVI mass in this area extended the ability to treat ZVI longer than in other areas. These overall dissolution data suggest that supplying sufficient ZVI mass to locations of high TCE source mass is critical, as expected. The extent of TCE rebound is an indication of how significantly the ZVI reduced the TCE mass before being expended. The ZVI treatment appears to have been sufficient to reduce most of the TCE mass during the treatment period because the TCE rebound is insignificant compared to the initial TCE concentrations. At other locations, some rebound was observed, but at generally low concentrations (Truex, 2011).

### 6.3 SUMMARY OF PERFORMANCE RELATED TO OBJECTIVES

**Table 14. Summary of achievement of demonstration performance objectives.**

Type of Performance Objective	Primary Performance Criteria	Expected Performance (Metric)	Actual Performance Objective Met?	
			ZVI	ISB
Qualitative	Induce dechlorination of chlorinated ethenes.	Dechlorination to desired endpoints will be achieved in each treatment cell.	Reductive dechlorination was achieved through abiotic reactions with the formation of ethene and ethane and biotic reactions with the formation of DCE.	Reductive dechlorination was achieved biotically converting TCE to DCE during Phase 2 and to DCE, VC and ethene during Phase 3.
	Reduction in parent compounds and accumulation of abiotic and/or biotic reductive daughter products.	Biotic contaminant removal will be the primary mechanism at ambient and elevated temperature in the ISB test cell. Abiotic and biotic contaminant removal will be significant in the ZVI test cell at ambient temperature; however, abiotic mechanisms will predominate at elevated temperature.	Abiotic and biotic dechlorination products observed for both ambient and elevated temperature.	Biotic contaminant removal was the primary mechanism at ambient and elevated temperature in the ISB test cell
Quantitative	Characterize nature of contamination with test cell.	Sufficient contaminant mass will be present in both test cells to meet demonstration objectives.	Initial TCE soil concentration averaged 115 mg/kg near INJ, estimated 1 kg total TCE in test cell (10 mg/kg average concentration)	Initial TCE soil concentration averaged 32 mg/kg with maximum concentrations of 130 mg/kg near ISB-MW2.

**Table 14. Summary of achievement of demonstration performance objectives (continued).**

Type of Performance Objective	Primary Performance Criteria	Expected Performance (Metric)	Actual Performance Objective Met?	
Quantitative (continued)	Define rate of dechlorination as a function of temperature.	The rate of dechlorination will be enhanced at elevated temperature in both test cells relative to ambient temperature.	Rates at T>30C were higher than 10C by a factor of 4 based on dechlorination daughter products and a factor 8 using chloride.	Modeled rates based on empirical correlation at T=40C were higher than 10C by a factor of 3.6 based on dechlorination daughter products and a factor of 5.3 using chloride.
	Quantify test cell mass balance and loss mechanisms for chlorinated ethenes in the test cells as a function of temperature.	Contaminant mass removal will be enhanced at elevated temperature in both test cells relative to ambient temperature.	TCE mass loss = 9 mg/kg with 85% of loss at T>30C with volatilization accounting for less < 1% of losses based on modeling.	TCE treatment rate increased by a factor of 4.6 at T=40C compared to 10C based on empirical correlation. Most advective transport in groundwater with volatilization accounting for <1.45% of losses.
	Evaluate cost-effectiveness of heating.	The overall treatment efficiency at elevated temperature will be enhanced sufficiently to offset the cost of heating in both test cells.	ZVI cost = \$626K ZVI+heat cost = \$632K High Temp. Thermal=\$692K	ISB cost = \$599K ISB+heat cost = \$567K High Temp. Thermal=\$692K

*This page left blank intentionally.*

## 7.0 COST ASSESSMENT

### 7.1 COST MODEL

A cost model for the project was developed in order to benefit professionals who may consider similar technology at other sites. While costs may vary depending on site size, location, subsurface conditions, etc., the cost model details all the assumptions from which specific cost elements were based. Many of the assumptions pertain to labor expenditure rates and project scale. Figure 18 illustrates the assumptions for the ZVI treatment area and system infrastructure used for the cost model. Figure 19 illustrates the assumptions for the ISB treatment area and system infrastructure for the cost model. Table 15 provides details of the cost model treatment volume. Incremental costs for adding low-temperature ISB or ZVI was evaluated under the assumption that high-temperature thermal system was operated. There are several applications for how the technologies could be combined including:

- Implementation of low-temperature heating with ISB or ZVI as a stand-alone technology,
- Implementation of low-temperature heating with ISB or ZVI in conjunction with high-temperature thermal to address areas around the high-temperature thermal treatment zone where it is not cost-effective to treat with high temperature thermal,
- Implementation of low-temperature heating with ISB or ZVI in conjunction with high-temperature thermal as a polish following treatment.

To evaluate the technologies, a model system was developed. Table 15 provides a real and depth of treatment dimensions of the model system, and a starting target-zone contaminant mass to evaluate treatment rates and durations in the model system. The model assumptions for in situ treatment based on the demonstration are as follows:

- Enhanced in situ treatment rates at elevated temperatures were primarily driven by enhanced dissolution due to increased temperatures relative to ambient treatment temperatures,
- The in situ treatment technologies can treat contaminants mobilized from the source at temperatures up to 50°C effectively in the saturated zone,
- Contaminants transported to the vadose zone during low-temperature heating did not require additional treatment to address.

The model treatment zone dimensions are 40 ft (12.2 meters [m]) in length, 40 ft (12.2 m) in width, and 30 ft (9.1 m) in depth, for a total treatment volume of 1,778 cubic yards (1,360 m<sup>3</sup>). Additionally, an initial chloroethene contaminant mass of 40 kg is assumed. Treatment rates were based on modeling for the high temperature thermal and for dissolution of NAPL and with enhancement factors at elevated temperatures demonstrated in this project. The assumptions are as follows:

- A high temperature thermal treatment rate of 470 g/d was used to estimate a total treatment duration of 85 days.

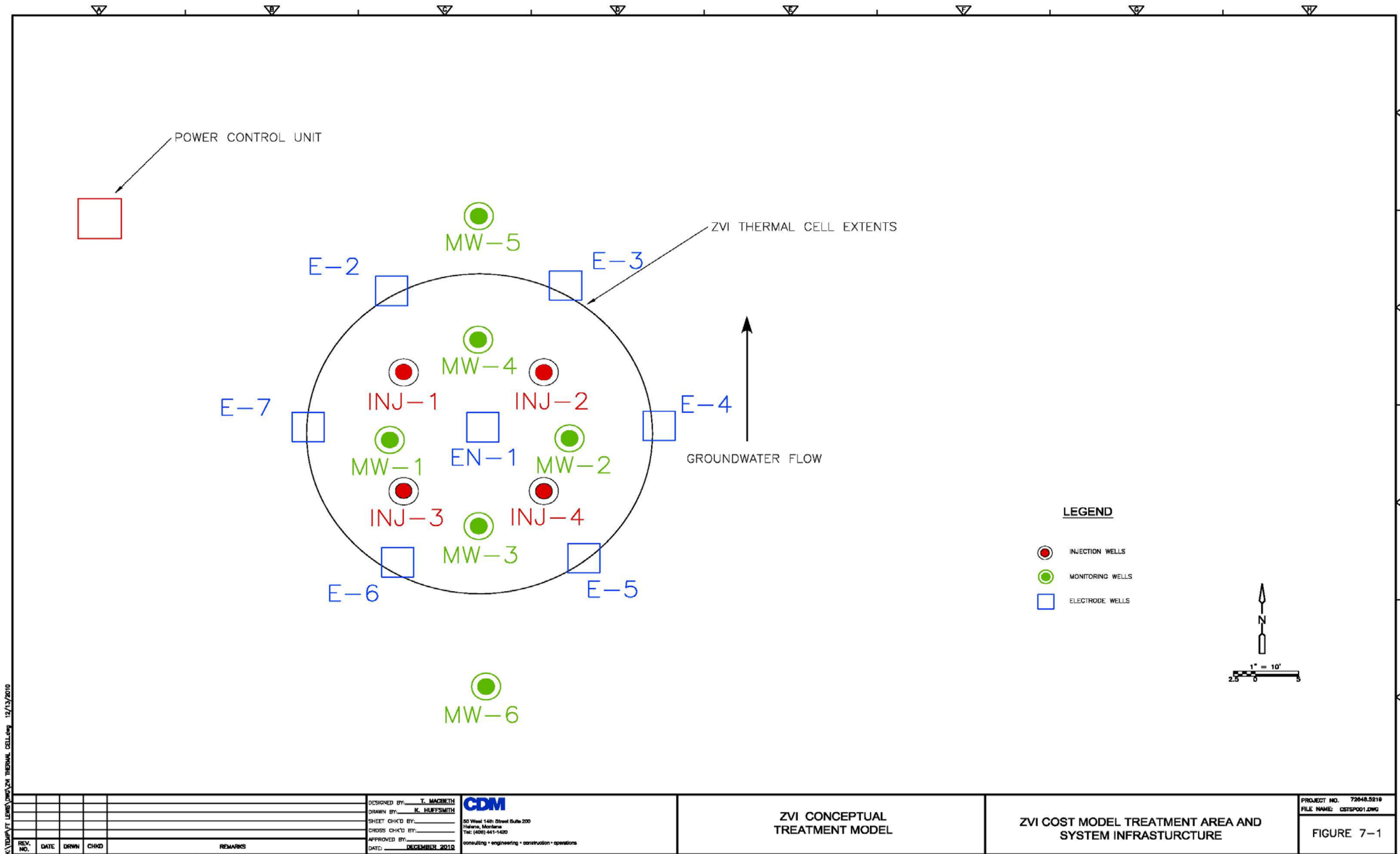


Figure 18. ZVI cost model treatment area and system infrastructure.

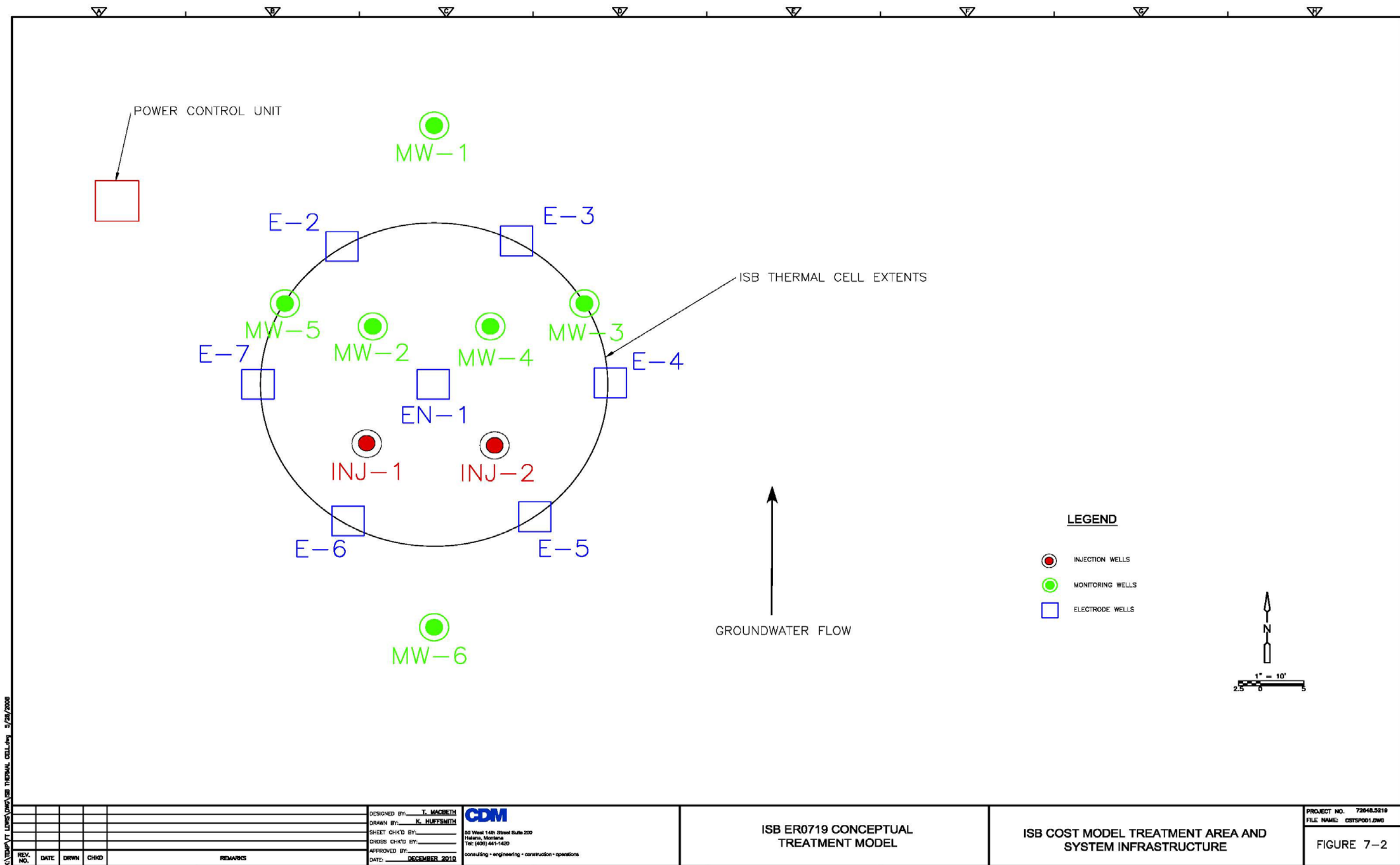


Figure 19. ISB cost model treatment area and system infrastructure.

- Energy consumptions were based on energy consumed during the demonstration for the ISB and ZVI.
- Treatment rates for both ISB and ZVI under ambient temperatures are assumed to be the same. The timeframe for dissolution of all 40 kg of the DNAPL is approximately 11 years assuming that the mass discharge rate is constant.
- For the low temperature ISB, the enhanced treatment rate factor was assumed to be 6 based on the assumption of a 40°C operating temperature, giving a treatment duration of approximately 1.8 years.
- For the low temperature ZVI, the enhanced treatment rate factor was assumed to be a factor of 8 greater than ambient temperatures based on the assumption of a 50°C operating temperature, giving a treatment duration of approximately 1.3 years.
- Ambient mass discharge rates out of the treatment zone are:

$$J=VaC \quad Md = \sum JA$$

Where J is the contaminant mass flux, Va is the Darcy velocity, C is the contaminant concentration, Md is the mass discharge and A is the treatment area transect. It is assumed that Va= 0.3 ft per day and average concentration across the treatment zone transect is 1,000 ug/L TCE giving an ambient temperature mass discharge rate of 10 grams TCE per day. Figure 20 illustrates the treatment times for the four treatment scenarios using these assumptions.

**Table 15. Cost assumption model.**

<b>Model Treatment Volume Dimensions</b>		
<b>Treatment Zone Dimensions and Volume</b>		
N	0.25 --	total porosity estimated from previous data
Ne	0.18 --	effective porosity from tracer test
L	12.2 m	treatment zone length
W	12.2 m	treatment zone width
H	9.1 m	length of filter pack
x sectional area	0 m <sup>2</sup>	for total inflow/outflow
plan view area	148.7 m <sup>2</sup>	for volatilization
Vt	1360 m <sup>3</sup>	total volume
<b>Treatment Zone Mass</b>		
Bulk dens.	1900 kg/m <sup>3</sup>	
Total mass	40 kg	
Ambient Rate	213 g/d	
Heated Rate	470 g/d	
Time to Treat	85 days	

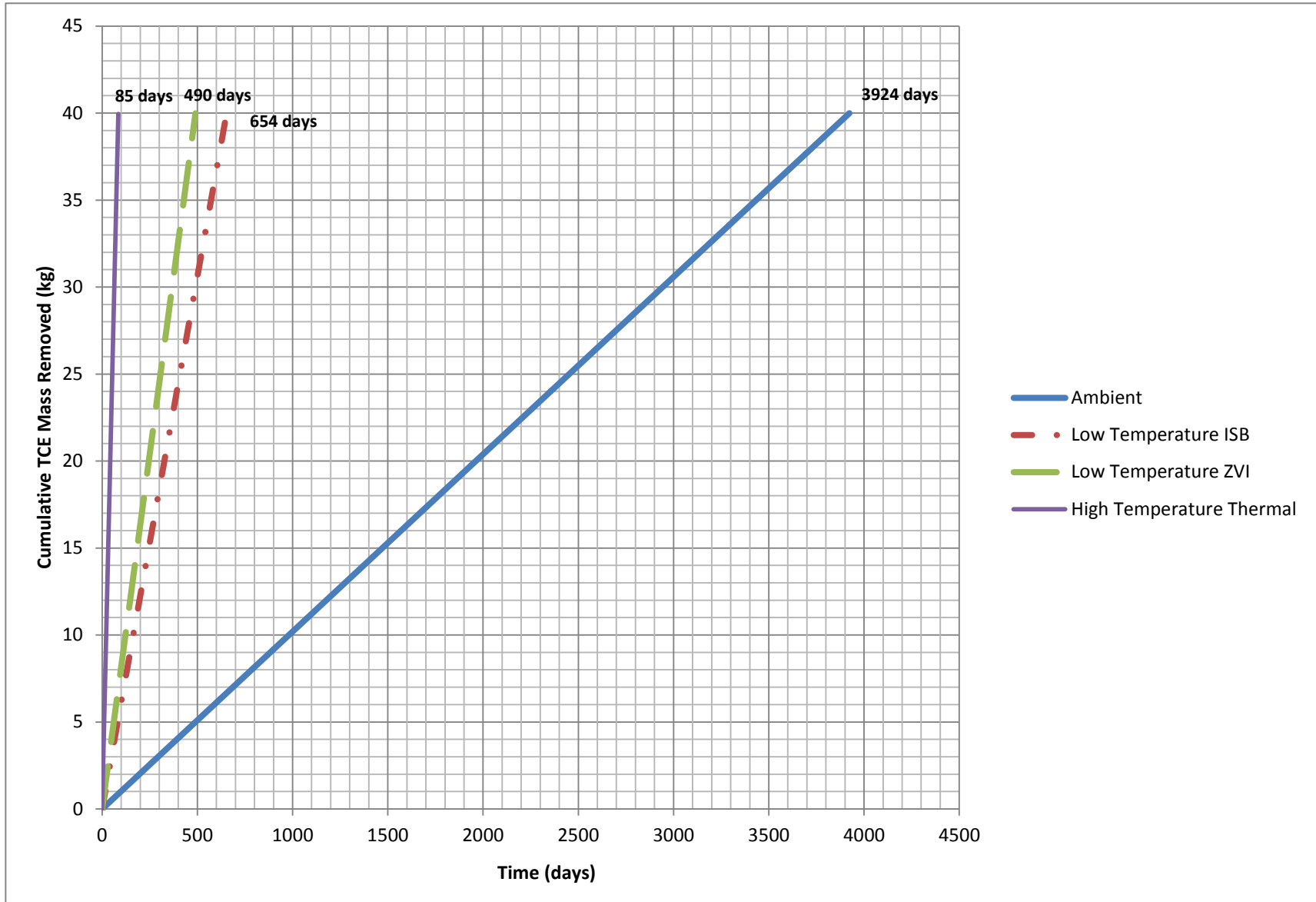


**Figure 20. Treatment time comparison.**



For each cost element, cost data was tracked during the life cycle of the demonstration, and was captured in the model. Table 16 details a comparison between costs of ZVI combined with low temperature thermal. Table 17 details a comparison between costs for ISB combined with low temperature thermal. Table 18 details all of the cost elements and sub-categories associated with high temperature ERH to compare to the low temperature applications. Costs have been divided into the common cost elements of 1) start-up, 2) capital, 3) operation and maintenance, 4) demobilization, and 5) waste disposal. Additional detail regarding assumptions for the cost model is provided in the Final ER-0719 Work Plan (CDM Smith, 2012).

## **7.2 COST DRIVERS**

### **7.2.1 ZVI**

Emplacement is a cost element that needs to be considered for ZVI applications. ZVI has been used for a number of different applications and using several different methods for emplacing it in the targeted treatment zone. In this work, we demonstrated direct injection of ZVI into an aquifer using a shear-thinning fluid to facilitate ZVI distribution. Cost for injection may increase in steps for thicker zones because multiple injection screens/wells may be needed to facilitate more uniform vertical distribution of the ZVI. Thus, for emplacement costs, the likely range for injection well spacing is on the order of 3 to 8 m. Costs associated with the injection process are expected to be similar to injection of ISB amendments, but with somewhat different equipment.

ZVI material cost is another factor for the technology, because the ZVI was injected, a uniform small particle size ZVI material was necessary (Oostrom, 2007). A carbonyl ZVI micropowder used in this demonstration, however, its cost is about 3 times higher than ZVI materials more typically used for trenching or soil mixing applications. The thermally enhanced ZVI approach is likely more appropriate for a source area with single to low 10s of mg/kg contaminant concentrations due to the cost implications of high dosing required for higher contaminant concentrations.

As illustrated above, the thermally enhanced ZVI process proceeds rather rapidly, compared to ambient temperature treatments, so the monitoring requirements for thermally enhanced ZVI would be much lower. Additionally, the monitoring intensity for appropriate thermally enhanced ZVI applications would be lower than for standard thermal treatment of the same target because much less process control and associated monitoring is necessary.

Based on the demonstration results, heating to 40oC is likely sufficient for TCE contamination. A standard ERH approach was used to provide the heating for the demonstration. Optimization of this heating system may result in some cost savings compared to the heating cost basis used for the cost estimate herein.

**Table 16. Cost model assumptions and costs for low-temperature ZVI.**

<b>Cost Element</b>	<b>Sub-category</b>	<b>Detail</b>	<b>Costs</b>
START-UP COSTS	<b>Design</b>	Design, Permits	<b>\$36,000</b>
	<b>- Field Preparation</b> (includes contracting for sampling and drilling, drilling costs [two mobilizations] and permitting).	<b>Total:</b> Senior Engineer- 35 hr/ \$125 per hr Geologist- 120 hr/ \$110 per hr Field Technician- 120 hr/ \$80 per hr Subcontract (Drilling)- \$62/ft for 7 electrodes to 37 ft, and 1 TMP, to 25 ft and \$84/ft for 8 injection/MWs at 30 ft Misc. (forklift rental, boring logs, survey and utility locate)	<b>\$85,623</b> \$4375 \$13,200 \$9600 \$38,448 \$5000
	<b>Preliminary Site Characterization:</b> - Hydraulic Testing including a tracer injection test and associated labor, equipment and materials	Tracer/Pump Test	\$15,000
CAPITAL COSTS	<b>Heating System Installation</b>	<b>Total:</b>	<b>\$175,000</b>
		Vapor Cap Electrode Materials Mobilization (security system and downhole electrodes) Vapor Treatment System Installation Thermal Subsurface Installation Surface Installation (PCU and electrical connections) and Startup Electrical Permit and Utility Connection to PCU	- \$50,000 - \$12,000 \$78,000 \$35,000
OPERATION AND MAINTENANCE COSTS	<b>Heating System Operations and Maintenance (O&amp;M)</b>	<b>Total:</b>	<b>\$76,560</b>
		Thermal Remediation System Operation Electrical Energy Usage (assume \$0.08/kWh for 170 MWh) Other operational costs including vapor sampling of the above-ground vapor treatment system Carbon Usage, Transportation & Regeneration associated with above-ground vapor treatment system Operational Monitoring Costs	\$36,660 \$36,400 - \$3500
	<b>Oversight:</b> - project management, routine reporting, regulatory interface, and technical oversight for 1.3years	Program Manager- 120 hr per year / \$140 per hr Senior Engineer- 300 hr per year / \$125 per hr Database Management- 100 hr per year/\$80 per hr	<b>\$78,590</b> \$21,840 \$48,750 \$8000

**Table 16. Cost model assumptions and costs for low-temperature ZVI (continued).**

<b>Cost Element</b>	<b>Sub-category</b>	<b>Detail</b>	<b>Costs</b>
OPERATION AND MAINTENANCE COSTS (continued)	<b>ZVI Injections:</b>		<b>\$124,592</b>
	- assume 4 injection wells, 2 injection events	Program Manager- 40 hr/ \$140 per hr	\$5600
	Each injection is 4 people for 2 days plus 4 people for 2 days setup prior to the overall injection event	Senior Engineer- 60 hr/ \$125 per hr	-
	Oversight is engineer for 60 hours, PM for 40 hours per event	Field Technician- 320 hr/ \$80 per hr	\$25,600
	ZVI bulk costs is \$9.35/lb for the injectable uniform 2 micron diameter iron used in the project. For injectability, only iron with characteristics similar to the iron used in the project is viable (see Truex et al. 2010).	Materials: ZVI (0.23% ZVI by wt soil or 4.1 kg ZVI/m3 soil)	\$86,592
	Capital Equipment Rental:	Subcontract (ZVI Injection System)= \$1800/injection + \$5000 ancillary equipment	\$6800
	<b>Sampling and Analysis:</b>		<b>\$25,280</b>
	- VOC, geochemistry for 4 events over the short operational period. The last event is considered closure of the treatment	Program Manager- 16 hr/ \$140 per hr	\$2240
	Analytical Subcontract	Senior Engineer- 32 hr/ \$125 per hr	\$4000
		Senior Engineer- 32 hr/ \$125 per hr	\$4000
Field Technician- 160 hr/ \$80 per hr		\$12,800	
Subcontract (Analytical)- 6 monitoring locations, \$260/sample		\$6240	
DEMOBILIZATION	<b>Demobilization</b>		<b>\$23,960</b>
	Demobilization		\$21,000
	Well abandonment		<b>\$2960</b>
WASTE DISPOSAL		Disposal of Drill Cuttings and waste disposal	<b>\$7,100</b>
<b>GRAND TOTAL</b>			<b>\$632,705</b>

Assumptions: Assume that RI characterization is sufficient for treatment design and that minimal additional characterization during installation is used to finalize the design. Downgradient monitoring not included in the cost.

**Table 17. Cost model assumptions and costs for low-temperature ISB.**

<b>Cost Element</b>	<b>Sub-category</b>	<b>Detail</b>	<b>Costs</b>
START-UP COSTS	<b>Design - Field Preparation</b> (includes contracting for sampling and drilling, drilling costs [two mobilizations] and permitting).	Design, Permits	<b>\$36,000</b>
		<b>Total:</b>	<b>\$70,623</b>
		Senior Engineer- 35 hr/ \$125 per hr	\$4375
		Geologist- 120 hr/ \$110 per hr	\$13,200
		Field Technician- 120 hr/ \$80 per hr	\$9600
		Subcontract (Drilling)- \$62/ft for 7 electrodes to 37 ft, and 1 TMP, to 25 ft and \$84/ft for 8 injection/MWs at 30 ft	\$38,448
	Misc. (forklift rental, boring logs, survey and utility locate)	\$5000	
	<b>Preliminary Site Characterization:</b>	<b>Total:</b>	<b>\$15,000</b>
	- Hydraulic Testing- pump and tracer test	Tracer/Pump Test	\$15,000
	(includes pumping tests; four tracer tests; labor for sampling, all equipment, supplies, and tracers for four tracer tests).		
CAPITAL COSTS	<b>Heating System Installation</b>	<b>Total:</b>	<b>\$175,000</b>
		Vapor Cap	-
		Electrode Materials Mobilization (security system and downhole electrodes)	\$50,000
		Vapor Treatment System Installation	-
		Thermal Subsurface Installation	\$12,000
		Surface Installation (PCU and electrical connections) and Startup	\$78,000
		Electrical Permit and Utility Connection to PCU	\$35,000
OPERATION AND MAINTENANCE COSTS	<b>Heating System O&amp;M</b>	<b>Total:</b>	<b>\$88,460</b>
		Thermal Remediation System Operation	\$50,760
		Electrical Energy Usage (assume \$0.08/kWh for 130 MWh)	\$34,200
		Other operational costs including vapor sampling of the above-ground vapor treatment system	-
		Carbon Usage, Transportation & Regeneration associated with above-ground vapor treatment system	
		Operational Monitoring Costs	\$3500
		<b>Oversight:</b>	
	-project management, routine reporting, regulatory interface, and technical oversight for 1.8 years	Program Manager- 120 hr per year / \$140 per hr	\$30,240
		Senior Engineer- 300 hr per year / \$125 per hr	\$67,500
		Database Management- 100 hr per year/\$80 per hr	\$8000

**Table 17. Cost model assumptions and costs for low-temperature ISB. (continued).**

<b>Cost Element</b>	<b>Sub-category</b>	<b>Detail</b>	<b>Costs</b>
OPERATION AND MAINTENANCE COSTS (continued)	<b>Bioremediation Amendment Injections:</b>		<b>\$24,993</b>
	- assume 2 wells and 2 events for 1.8 year and 10% whey	Program Manager- 40 hr/ \$140 per hr	-
		Senior Engineer- 80 hr/ \$125 per hr	-
		Field Technician-100 hr/ \$80 per hr	\$8000
		Materials	\$13,393
	Capital Equipment Rental:	Subcontract (Whey Injection System)= \$1800/month/2X	\$3600
	<b>Sampling and Analysis:</b>		<b>\$20,120</b>
	- VOC, carbon, bioactivity, redox and DNA for 4 events	Program Manager- 20 hr/ \$140 per hr	\$2800
		Senior Engineer- 40 hr/ \$125 per hr	-
		Field Technician- 80 hr/ \$80 per hr	\$6400
Analytical Subcontract	Analytical- 8 monitoring locations, \$260/sample/ 4 sampling events, (molecular)- 4 sampling locations, \$325/sample/ 2 sampling events	\$10,920	
DEMOBILIZATION	<b>Demobilization</b>		<b>\$23,960</b>
	Demobilization	\$21,000	
	Well abandonment	\$2960	
WASTE DISPOSAL	Disposal of Drill Cuttings and waste disposal	\$7100	
<b>GRAND TOTAL</b>			<b>\$566,996</b>

Assumptions: Assume that RI characterization is sufficient for treatment design and that minimal additional characterization during installation is used to finalize the design. Downgradient monitoring not included in the cost.

## 7.2.2 ISB

The hydraulic conductivity of the treatment zone determines ISB injection well spacing, and the heterogeneous distribution of contaminants determines the vertical intervals that are targeted and the type of injection required to deliver amendments to the target vertical interval, and are therefore the major cost drivers for ISB treatment. In addition, hydraulic conductivity and heterogeneity would determine the required spacing for the heating electrodes and also determine the power required to heat the treatment zone to the desired temperature. However, given the Landfill 2 was a worst case scenario, it is the opinion of the project team that hydraulic control would likely not be required to implement this technology at most sites.

Similarly, the total mass of residual contamination can be a cost driver. As long as the source consists primarily of solvents at residual saturation or sorbed to the soil, mass removal can be fairly rapid subject to the potential constraints of hydraulic conductivity and heterogeneity discussed above. However, if DNAPL is present in pools, cleanup timeframe becomes limited by dissolution rates. While low temperature ISB can enhance the mass transfer by a factor of more 5 to even 10 or higher, large pools of DNAPL could still require decades to dissolve, driving costs up significantly. Another potential cost driver is hydraulic containment or development of a treatment zone large enough to allow for effective degradation of dissolved chlorinated solvents. If a sufficient downgradient buffer zone is not available at a site and extraction of groundwater is required to prevent the temporary increase in mass flux caused by thermal heating from impacting some nearby downgradient receptor, costs would increase. A fourth potential cost

driver is vapor intrusion. Although this demonstration indicated that volatilization was a small fraction of the total mass discharge from the treatment zone, if conditions of the treatment zone allowed for significant VOC concentrations to accumulate, and SV extraction was required, this would also increase technology costs.

**Table 18. Cost model assumptions and costs for high-temperature thermal.**

<b>Cost Element</b>	<b>Sub-category</b>	<b>Detail</b>	<b>Costs</b>	
START-UP COSTS	<b>Design</b>	Design, Permits	<b>\$40,000</b>	
	<b>- Field Preparation</b>	<b>Total:</b>	<b>\$65,175</b>	
	(includes contracting for sampling and drilling, drilling costs [two mobilizations] and permitting).		Senior Engineer- 35 hr/ \$125 per hr	\$4375
			Geologist- 120 hr/ \$110 per hr	\$13,200
			Field Technician- 120 hr/ \$80 per hr	\$9600
			Subcontract (Drilling)- \$62/ft for 7 electrodes to 37 ft, and 1 TMP, to 25 ft and \$84/ft for 8 injection/MWs at 30 ft	\$33,000
			Misc. (forklift rental, boring logs, survey and utility locate)	\$5000
	<b>Preliminary Site Characterization:</b>	<b>Total:</b>	<b>\$15,000</b>	
- Hydraulic Testing- pump and tracer test	Tracer/Pump Test	\$15,000		
(includes pumping tests; four tracer tests; labor for sampling, all equipment, supplies, and tracers for four tracer tests).				
CAPITAL COSTS	<b>Heating System Installation</b>	<b>Total:</b>	<b>\$238,000</b>	
		Vapor Cap	-	
		Electrode Materials Mobilization (security system and downhole electrodes)	\$63,000	
		Vapor Treatment System Installation	-	
		Thermal Subsurface Installation	\$12,000	
		Surface Installation (PCU and electrical connections) and Startup	\$128,000	
		Electrical Permit and Utility Connection to PCU	\$35,000	
OPERATION AND MAINTENANCE COSTS	<b>Heating System O&amp;M</b>	<b>Total:</b>	<b>\$187,000</b>	
		Thermal Remediation System Operation	\$133,000	
		Electrical Energy Usage (assume \$0.08/kWh for 350MWh)	\$30,000	
		Other operational costs including vapor sampling of the above-ground vapor treatment system	-	
		Carbon Usage, Transportation & Regeneration associated with above-ground vapor treatment system	\$13,000	
		Operational Monitoring Costs	\$11,000	

**Table 18. Cost model assumptions and costs for high-temperature thermal (continued).**

<b>Cost Element</b>	<b>Sub-category</b>	<b>Detail</b>	<b>Costs</b>
OPERATION AND MAINTENANCE COSTS (continued)	<b>Oversight:</b>		<b>\$62,300</b>
	-project management, routine reporting, regulatory interface, and technical oversight	Program Manager- 120 hr per year / \$140 per hr	\$16,800
		Senior Engineer- 300 hr per year / \$125 per hr	\$37,500
		Database Management- 100 hr per year/\$80 per hr	\$8,000
	<b>Sampling and Analysis:</b>		<b>\$39,120</b>
	- VOC, carbon, bioactivity, redox for 4 events	Program Manager- 20 hr/ \$140 per hr	\$2,800
		Senior Engineer- 40 hr/ \$125 per hr	\$12,600
		Field Technician- 160 hr/ \$80 per hr	\$12,800
Analytical Subcontract	Analytical- 8 monitoring locations, \$260/sample/ 4 sampling events, (- 4 sampling locations, \$325/sample/ 2 sampling events	\$10,920	
DEMOBILIZATION	<b>Demobilization</b>		<b>\$39,960</b>
	Demobilization		\$37,000
	Well abandonment		<b>\$2,960</b>
WASTE DISPOSAL		Disposal of Drill Cuttings and waste disposal	<b>\$3,000</b>
<b>GRAND TOTAL</b>			<b>\$692,515</b>

Assumptions: Assume that RI characterization is sufficient for treatment design and that minimal additional characterization during installation is used to finalize the design. Downgradient monitoring not included in the cost.

### 7.2.3 Thermal

The cost drivers for the in situ heating system were the size of the treatment area, the power control unit (PCU) and electrical system available, and the availability of power. Less expensive systems could be developed for low-temperatures applications decreasing the cost for treatment.

## 7.3 COST ANALYSIS

A summary of cost factors for low-temperature ZVI and ISB is presented in Tables 16 and Table 17. For comparison an estimate of high temperature heating was also provided in Table 18. These data suggest that low-temperature heating is less expensive than high temperature ERH, but only incrementally so, and due to the slower mass removal rates, likely makes sense only for sites that contain only low to moderate VOC concentrations. However, the benefit of heating to in situ reactions was clearly demonstrated both from an enhanced kinetics of degradation reactions and VOC mass removal rates. Therefore, combining in situ treatment with heating, especially for sites already considering high temperature heating, may provide added benefit. This is especially true for areas around and/or downgradient of the high concentration “core” of the source area outside high-temperature ERH treatment makes sense, but still contains high concentrations of VOCs in soil or groundwater. In addition, in situ technologies could be implemented after thermal shut down to treat any remaining contaminants in the treatment zone.

## 8.0 IMPLEMENTATION ISSUES

The controlling factors for implementation of thermally enhanced ISB or ZVI as demonstrated are 1) subsurface properties related to injection of the amendments, 2) contaminant type and associated reaction kinetics, 3) contaminant concentrations and the associated amendment dosing requirements, and 4) targeted treatment volume. As shown in the field demonstration, the thermally enhanced ZVI approach appears to be less impacted by groundwater flow velocity than other in situ technologies, including ISB using soluble amendments, due to the favorable fluid properties of the shear-thinning fluid and the static nature of the ZVI reaction catalyst.

Injected ZVI particles travel in the subsurface until they are filtered due to physical interaction with the sediment (e.g., contacting pores smaller than the particle size) or until the particles settle and are no longer suspended in the carrier fluid. ZVI injection with a shear-thinning fluid and surfactant components is designed to maximize ZVI particle transport by slowing the settling time of the particles (Oostrom 2007). The viscosity of the fluid slows particle settling. Additionally, the surfactant helps prevent agglomeration of particles, which prevents enhanced settling. Filtration processes are minimized through use of a relatively small ZVI particle size (nominally 2 micron diameter particles).

As with other in situ treatment process that require fluid injection of amendments to the subsurface, the subsurface properties impact the injection process. Carrier fluid distribution and injection flow and pressure are impacted by sediment permeability and heterogeneity. Permeability constraints on fluid injection for ZVI are similar to those for other in situ technologies like bioremediation in that the injection fluid will tend to follow higher permeability pathways and injection into silt and finer materials will likely not be possible due to pressure constraints. For ZVI injection the particle size distribution and associated pore size distribution of the sediment will provide additional constraints due to filtration processes that are not present for solute injection. A reasonable portion of the porosity needs to be significantly greater than the 2-micron diameter of the ZVI particles. A similar type of constraint is typically considered for emulsified oil injection. For sites with small sediment pore sizes, injection of micron scale ZVI may be precluded. Use of nano-scale ZVI could be considered as an alternative to enable distribution of ZVI in these cases and has the potential to offer similar treatment benefits when coupled with heating. However, specific data for nano-scale iron was not collected in this demonstration and the beneficial aspects of nano-scale ZVI (high reactivity, enhanced particle delivery) along with the potential drawbacks (cost, retention in sediment, short-lived reactivity) would need to be considered for this alternative approach.

The reaction kinetics and daughter products of TCE dechlorination by ZVI and ISB were quantified in this project for the field test site. The kinetics and product distribution were shown to be enhanced by heating and favorable for relatively rapid treatment of moderate source contaminant concentrations as were present at the field test site and used for the cost evaluation. The specific contaminants, concentrations, and groundwater geochemistry at a specific site will impact the dechlorination reaction kinetics. Thus, either a review of literature (for resources, see Section 9 and Truex 2010, 2011) to identify appropriate reaction kinetics or a focused laboratory treatability study as was conducted for this field demonstration would be needed to evaluate the effectiveness of thermally enhanced in situ treatment options for a specific site and as input to the treatment design.



The ZVI dosing (i.e., the mass of ZVI that needs to be delivered to the treatment zone) is a function of the total contaminant mass that needs to be treated (i.e., contaminant concentration in water and associated with NAPL or sediments multiplied by the treatment volume). Often, it is difficult to accurately estimate the contaminant mass within the treatment zone. Thus, an estimate from available data and use of a “safety factor” increase may be needed to calculate the ZVI dosing that will be sufficient. It may also be effective to make an initial ZVI dosing selection with the realization that a second injection can be used later if needed based on initial treatment results. There should be no major constraints to conducting multiple ZVI injections if needed unless the sediment conditions show that strong filtration of ZVI particles occurred near the injection well. As the contaminant mass increases, so does the ZVI dosing requirement increase. Two ultimate constraints related to contaminant mass may limit the applicability of the thermally enhanced ZVI. First, the concentration of ZVI in the injection stream is likely limited to a few weight percent ZVI in order for the fluid to carry the ZVI into the subsurface. The ZVI concentration in the injection fluid for the demonstration was about 1.4 wt %. As the ZVI concentration increases, problems with injection solution mixing and particle agglomeration may occur. The maximum ZVI concentration possible in the injection solution was not determined in this demonstration, but it is likely that concentrations significantly higher than 1.4 wt% will not work. Second, as the ZVI dosing requirement increases, the ZVI material costs increase. At some point, these material costs will render the thermally enhanced ZVI costs to be unfavorable relative to other technologies, in particular, at high contaminant concentrations, standard thermal treatment may become a preferred option.

For ISB, the key injection consideration was longevity and retention of the amendments within the target treatment zone. Increasing temperatures enhanced both the rate of amendment utilization and contaminant degradation. However, generally the biomass was more efficient at higher temperatures. In this demonstration, the dosing of whey was maintained constant during the ambient and heated phases, and the dechlorination was considerably enhanced, even with increased amendment utilization. Therefore, it is not the opinion of the project team that increased amendment dosing is required at elevated temperatures. However, retention of amendments was an issue at Landfill 2 due to extremely high groundwater velocities. While Landfill 2 represented a worst case scenario, both distribution and retention of amendments is a key design consideration. Of note, is that the requirement for carbon will likely be much smaller at most sites compared to Landfill 2. The majority of the amendment injected at Landfill 2 was lost due to advective transport out of the target treatment area. Therefore, the amount of amendment needed in the treatment zone would be a fraction (likely an order of magnitude less) at sites with slower groundwater velocities compared to the injection strategy implemented at Landfill 2.

Implementation of thermally enhanced ZVI and ISB treatment is impacted by the size of the targeted treatment volume. As with all treatment technologies, cost and implementation processes are a function of the treatment volume. In particular for the ZVI and ISB, the size will impact the design of the injection wells (screen length, spacing, total number) and layout of the heating infrastructure. The ZVI technology, while scalable, may not be as conducive to large volumes (i.e., more than 2 or 3 times the size used for the cost estimate case study) whereas technologies such as ISB that use solute amendments that are more readily distributed over large volumes.

## 9.0 REFERENCES

- 40 CFR 141.61, 2002, Title 40, "Protection of Environment," Subchapter D, "Water Programs," Part 141, "National Primary Drinking Water Regulations," Section .61, "Maximum Contaminant Levels for Organic Contaminants," Code of Federal Regulations, Office of the Federal Register.
- Arnold, W. A., Roberts, A. L. 2000. Pathways and kinetics of chlorinated ethylene and chlorinated acetylene reaction with Fe(0) particles. *Environ. Sci. Technol.* 2000, 34, 1794-1805.
- Atlas, R.M., and R. Bartha. 1987. *Microbial Ecology: Fundamentals and Applications*. The Benjamin/Cummings Publishing Company, Inc., Menlo Park, California.
- Bouwer, E. J.; McCarty, P. L. 1983. *Appl. Environ. Microbiol.* 45, 1286-1294.
- Cantrell, K.J., D.I. Kaplan, and T.J. Gilmore. 1997a. Injection of colloidal size particles of Fe0 in porous media with shear thinning fluids as a method to emplace a permeable reactive zone. *Land Contamination and Reclamation*, 5:253-257.
- Cantrell, K.J., D.I. Kaplan, and T.J. Gilmore. 1997b. Injection of colloidal Fe0 particles in sand with shear-thinning fluids. *J. Environ. Eng.* 123:786-791.
- Carr, C. S.; Garg, S.; Hughes, J. B. 2000. Effect of dechlorinating bacteria on the longevity and composition of PCE-containing nonaqueous phase liquids under equilibrium dissolution conditions. *Environ. Sci. Technol.* 2000, 34 (6), 1088-1094.
- CDM Smith. 2012. Final Report ER-0179. Combining Low-Energy Electrical Resistance Heating with Biotic and Abiotic Reactions for Treatment of Chlorinated Solvent DNAPL Source Areas.
- Ebert, M., R. Kober, A. Parbs, V. Plagentz, D. Schafer, and A. Dahmke. 2006. Assessing degradation rates of chlorinated ethylenes in column experiments with commercial iron materials used in permeable reactive barriers. *Environ. Sci. Technol.* 40:2004-2010
- EPA. 2004. "Cleaning Up the Nation's Waste Sites: Markets and Technology Trends," EPA 542-R-04-015, Environmental Protection Agency, Office of Solid Waste and Emergency Response, September 2004.
- ER-0218. 2003. Demonstration Plan for In Situ Bioremediation of Chlorinated Solvents with Enhanced Mass Transfer at the Fort Lewis East Gate Disposal Yard, Prepared by North Wind, Inc., NWI-ID-2002-048, for the Environmental Security Technology Certification Program, January 2003.
- ER-0318. 2004. Demonstration Plan for Applying Diagnostic Tools for Performance Evaluation of In Situ Bioremediation of a Chlorinated Solvent Source Area at the Fort Lewis East Gate Disposal Yard, Prepared by North Wind, Inc., NWI-ID-2004-029, for the Environmental Security Technology Certification Program, March 2004.

- Grant, G. P.; Kueper, B. H. 2004. The influence of high initial concentration aqueous-phase TCE on the performance of iron wall systems. *J. Contam. Hydrology*. 2004, 74, 299-312.
- Heath, W.O. and M.J. Truex. 1994. "Enhanced In Situ Bioremediation Using Six-Phase Electrical Heating." In: *In-Situ Remediation: Scientific Basis for Current and Future Technologies, Part 2*, G. W. Gee and N. R. Wing (eds.), Battelle Press, Richland, Washington, p. 781-797.
- Hendrickson, E. R.; Payne, J. A.; Young, R. M.; Starr, M. G.; Perry, M. P.; Fahnestock, S.; Ellis, D. E.; Ebersole, R. C. 2002. Molecular analysis of Dehalococcoides 16S ribosomal DNA from chloroethene-contaminated sites throughout North America and Europe. *Appl. Environ. Microbiol.* 2002, 68 (2), 485-495.
- Holliger, C; Schraa, G.; Stams, A. J.; Zehnder, A. J. 1993. A highly purified enrichment culture couples the reductive dechlorination of tetrachloroethene to growth. *Appl. Environ. Microbiol.* 1993, 59, 2991-2997.
- Horvath, A. R. 1982. Halogenated Hydrocarbons: Solubility-miscibility with water; Marcel Dekker: New York. NY, 1982.
- Imhoff, P. T.; Gleyzer, S. N.; McBride, J. F.; Vancho, L. A.; Okuda, I.; Miller, C. T. 1995. Cosolvent-enhanced remediation of residual dense nonaqueous phase liquids: Experimental investigation. *Environ. Sci. Technol.* 1995, 29 (8), 1966-1976.
- Imhoff, P. T.; Frizzell, A.; Miller, C. T. 1997. An evaluation of thermal effects on the dissolution of a nonaqueous phase liquid in porous media. *Environ. Sci. Technol.* 1997, 31 (6), 1615-1622.
- Interstate Technology Regulatory Council (ITRC). 2005. Permeable reactive barriers: lessons learned/new directions. Report # PRB-4. Washington DC: Interstate Technology and Regulatory Council, Permeable Reactive Barriers Team.
- Johnson, J. C.; Sun, S.; Jaffe, P. R. 1999. Surfactant enhanced perchloroethylene dissolution in porous media: The effect on mass transfer rate coefficients. *Environ. Sci. Technol.* 1999, 33 (8), 1286-1292.
- Kohn, T., and A.L. Roberts. 2006. The effect of silica on the degradation of organohalides in granular iron columns. *J. Contam. Hydrology* 83:70-88
- Kohring, G W, Rogers, J. E.; Wiegel, J. 1989. Anaerobic biodegradation of 2,4-dichlorophenol in freshwater lake sediments at different temperatures. *Appl. Environ. Microbiol.* 1989, 55, 348-353.
- Lee, P. K., Macbeth, T. W., Sorenson, K. S., Deeb, R. A. and Alvarez-Cohen, L. 2008. "Quantifying Genes and Transcripts To Assess the In Situ Physiology of Dehalococcoides spp. in a Trichloroethene-Contaminated Groundwater Site," *Appl. Environ. Microbiol.* 74: 2728-2739.

- Lee, P. K.H., Warnecke F., Brodie E., Macbeth T.W., Conrad M.E., Andersen G., and L. Alvarez-Cohen. 2012 “Phylogenetic Microarray Analysis of a Microbial Community Performing Reductive Dechlorination at a TCE-Contaminated Site.” *Environ. Sci. Technol.* 46(2):1044-1054.
- Lin, C.J. and S. Lo. 2005. Effects of iron surface pretreatment on sorption and reduction kinetics of trichloroethylene in a closed batch system. *Water Research.* 39:1037-1046.
- Macbeth, T. W., Harris, K. S.; Rothermel, J. S.; Wymore, R.; Sorenson, K. S.; Nelson, L. 2006. Evaluation of whey for bioremediation of trichloroethene source zones. *Bioremed. J.* 2006, 10 (3), 115-128.
- Mackay, D.; Shiu, W. Y.; Ma, K.; Lee, S. C. 2006. *Handbook of Physical-Chemical Properties and Environmental Fate for Organic Chemicals, second Ed. Chapter 5, Halogenated Aliphatic Hydrocarbons*; CRC Press, Taylor & Francis Group: Boca Raton, FL, 2006.
- Maymo-Gatell, X.; Chien, Y.; Gossett, J. M.; Zinder, S. H. 1997. Isolation of a bacterium that reductively dechlorinates tetrachloroethene to ethene. *Science.* 1997, 276 (5318), 1568-1571.
- Miehr, R., P.G. Tratnyek, J.Z. Bandstra, M.M. Scherer, M.J. Alowitz, E.J. Bylaska. 2004. Diversity of contaminant reduction reactions by zero valent iron: Role of the reductate. *Environ. Sci. Technol.* 38:139-147.
- Millington, R. J.; Quirk, J. P. Permeability of porous solids. 1961. *Trans. Faraday Soc.* 1961, 57 (7), 1200–1207.
- Oostrom, M, T.W. Wietsma, M.A. Covert, and V.R. Vermeul. 2005. Experimental Study of Micron-Size Zero-Valent Iron Emplacement in Permeable Porous Media Using Polymer-Enhanced Fluids. PNNL-15573, Pacific Northwest National Laboratory, Richland, Washington.
- Oostrom, M.; Wietsma, T. W.; Covert, M. A.; Vermeul, V. R. 2007. Zero-valent iron emplacement in permeable porous media using polymer additions. *Ground Water Monitoring and Remediation.* 2007, 27, 122-130.
- Orth, W.S. and Gillham, R.W. 1996. Dechlorination of trichloroethene in aqueous solution using Fe<sup>0</sup>. *Environ. Sci. Technol.* 30:66-71.
- Quinn, J., C. Geiger, C. Clausen, K. Brooks, C. Coon, S. O’Hara, T. Krug, D. Major, W-S. Yoon, A. Gavaskar, and T. Holdsworth. 2005. “Field Demonstration of DNAPL Dehalogenation Using Emulsified Zero-Valent Iron”. *Environ. Sci. Technol.*, 39(5):1309-1318.
- Reardon, E.J., 1995. Anaerobic corrosion of granular iron: Measurement and interpretation of hydrogen evolution rates. *Environ. Sci. Technol.* 1995, 29, 2936-2945.

- Roberts, A. L.; Totten, L. A.; Arnold, W. A.; Burris, D. R.; Campbell, T.J. 1996. Reductive elimination of chlorinated ethylenes by zero-valent metals. *Environ. Sci. Technol.* 1996, 30 (8), 2654-2659.
- Sale, T. 1998. Interphase Mass Transfer from Single Component DNAPLs. Ph.D. Dissertation, Colorado State University.
- Schnell, D.L. and J. Mack 2003. Installation of dispersed iron permeable reactive treatment zones using pneumatic injection. In: Chlorinated Solvent and DNAPL Remediation: Innovative Strategies for Subsurface Cleanup; Henry, S.M. and Warner, S.D., Eds.; Oxford University
- Sleep, B. E.; Ma, Y. 1997. Thermal variation of organic fluid properties and impact on thermal remediation feasibility. *J. Soil Contam.* 1997, 6 (3), 281-306.
- Sorenson, K. S. 2002. "Enhanced bioremediation for treatment of chlorinated solvent residual source areas". In: S. M. Henry, and S. D. Warner (eds), Innovative strategies for the remediation of chlorinated solvents and DNAPLs in the subsurface, p. 119-131. ACS Symposium Series 837, ACS Books, Washington, DC.
- Suyama, Akiko, Masaki Yamashita, Sadazo Yoshino, and Kensuke Furukawa. 2002. "Molecular Characterization of the PceA Reductive Dehalogenase of *Desulfitobacterium* sp. Strain Y51," *Journal of Bacteriology*, July 2002, p. 3419-3425, Vol. 184, No. 13.
- Szecsody, J., M. Williams, J. Fruchter, V Vermeul, and D. Sklarew. 2004. In situ reduction of aquifer sediments: Enhancement of reactive iron phases and TCE dechlorination. *Environ. Sci. Technol.* 38: 4656-4663.
- Truex, M. J.; Johnson, C. D.; Cole, C. R. *Numerical Flow and Transport Model for the Fort Lewis Logistics Center*; DSERTS NO. FTLE-33, Fort Lewis Public Works, Building 2102, Fort Lewis WA, 2006.
- Truex, M. J., Macbeth T. W., Vermeul, V. R., Fritz, B. G., Mendoza, M, D. P., Mackley R. D., Oostrom M., Wietsma T. W. . Sandberg, G., Powell, T., Powers, J. Pitre, E. Michalsen, M., Ballock-Dixon, S.J., and L. Zhong. 2011. Demonstration of Combined Zero-Valent Iron and Electrical Resistance Heating for In Situ TCE Remediation. *Environ. Sci. Technol.* 45, 5346–5351.
- Truex, M. J., Vermeul, V. R., Mendoza, M, D. P., Fritz, B. G., Mackley R. D., Oostrom M., Wietsma T. W. and Macbeth T. W. 2011. "Injection of Zero-Valent Iron into an Unconfined Aquifer Using Shear-Thinning Fluids." *Ground Water Monitoring & Remediation*: 31(1):50-58.
- Wadley S.L.S, R.W. Gillham, and L. Gui. 2005. Remediation of DNAPL source zones with granular iron: Laboratory and field tests. *Ground Water* 43(1):9-18.
- Yang, Y.; McCarty, P. L. "Biologically Enhanced Dissolution of Tetrachloroethene DNAPL." *Environ. Sci. Technol.* 2000, 34 (14), 2979-2984.

- Yaws, C. L. 2003. *Yaws' Handbook of Thermodynamic and Physical Properties of Chemical Compounds*; Knovel: Electronic ISBN 978-1-59124-444-8.
- Yaws, C. L.; Narasimhan P. K.; Gabbula C. 2009. *Yaws' Handbook of Antoine Coefficients for Vapor Pressure (2nd Electronic Edition)*; Knovel: Electronic ISBN 978-1-59124-879-8.
- Zhong, L., M. Oostrom, T.W. Wietsma, and M.A. Covert. 2008. Enhanced Remedial amendment delivery through fluid viscosity modifications: Experiments and numerical simulations. *J. Contam. Hydrol.* 101: 29-41, doi:10.1016/j.jconhyd.2008.07.007.

*This page left blank intentionally.*

## APPENDIX A

### POINTS OF CONTACT

<b>Point of Contact</b>	<b>Organization</b>	<b>Phone Fax E-Mail</b>	<b>Role In Project</b>
Tamzen Macbeth	CDM 50 West 14th Street Helena, MT, 59601	Phone: (208) 904-0238 Fax: (208) 904-0238 E-mail: macbethtw@cdmsmith.com	PI
Michael Truex	P.O. Box 999, MS K6-96 Richland, WA 99352	Phone: (509) 371-7072 E-mail: mj.truex@pnl.gov	Co-PI
Mandy Michalsen	4735 East Marginal Way South Seattle, WA 98134	Phone: (206) 764-3324 E-mail: Mandy.M.Michalsen@usace.army.mil	USACE Technical Lead
Tom Powell	Thermal Remediation Services (TRS) 4522 Muris Ln. Pasco, WA 99301	Phone: (509) 543-6192 E-mail: tpowell@thermalrs.com	Co-PI





**ESTCP Office**

4800 Mark Center Drive  
Suite 17D08  
Alexandria, VA 22350-3605

(571) 372-6565 (Phone)

E-mail: [estcp@estcp.org](mailto:estcp@estcp.org)  
[www.serdp-estcp.org](http://www.serdp-estcp.org)